

REWARD MODEL OVEROPTIMISATION IN ITERATED RLHF

000
001
002
003
004
005 **Anonymous authors**
006 Paper under double-blind review
007
008
009
010
011
012
013
014
015
016
017
018
019
020
021
022
023
024
025
026
027
028
029
030
031
032
033
034
035
036
037
038
039
040
041
042
043
044
045
046
047
048
049
050
051
052
053

ABSTRACT

Reinforcement learning from human feedback (RLHF) is a widely used method for aligning large language models with human preferences. However, RLHF often suffers from reward model overoptimisation, in which models overfit to the reward function, resulting in non-generalisable policies that exploit the idiosyncrasies and peculiarities of the reward function. A common mitigation is *iterated RLHF*, in which reward models are repeatedly retrained with updated human feedback and policies are re-optimised. Despite its increasing adoption, the dynamics of overoptimisation in this setting remain poorly understood. In this work, we present the first comprehensive study of overoptimisation in iterated RLHF. We systematically analyse key design choices: how reward model training data is transferred across iterations, which reward function is used for optimisation, and how policies are initialised. Using the controlled AlpacaFarm benchmark, we observe that overoptimisation tends to decrease over successive iterations, as reward models increasingly approximate ground-truth preferences. However, performance gains diminish over time, and while reinitialising from the base policy is robust, it limits optimisation flexibility. Other initialisation strategies often fail to recover from early overoptimisation. These findings offer actionable insights for building more stable and generalisable RLHF pipelines.

1 INTRODUCTION

Reinforcement learning from human feedback (RLHF) has become the standard method for aligning large language models with human preferences (Ziegler et al., 2020; Ouyang et al., 2022; Bai et al., 2022). However, RLHF faces a critical vulnerability: reward model overoptimisation (Gao et al., 2023). As fine-tuning progresses, models learn to overfit to the trained reward function - achieving high scores without genuinely satisfying human intent. This creates brittle policies that exploit loopholes rather than developing robust behaviours, leading to systems that appear aligned during training but fail catastrophically when deployed. Iterated RLHF represents a promising approach to combat this problem. By repeatedly collecting new preferences on the latest policy outputs, retraining the reward model, and fine-tuning the policy (Bai et al., 2022; Xiong et al., 2024), practitioners aim to iteratively close the gap between proxy and true reward. Despite its widespread adoption in industry (Ziegler et al., 2020; Ouyang et al., 2022; Bai et al., 2022), it remains uncertain whether iterated RLHF genuinely resolves overoptimisation, merely postpones the inevitable exploitation of the reward model akin to persistent adversarial policies (Gleave et al., 2020), or perpetuates a recurring cycle of overoptimisation in different forms (Singhal et al., 2024).

In this work, we present the first systematic investigation into reward model overoptimisation in iterated RLHF. We identify three pivotal design choices, highlighted in Figure 1, that critically influence the success or failure of the process: *preference data management* (i.e., whether to aggregate or isolate preference data across iterations), *reward function formulation* (i.e., the choice of reward signal to optimize in subsequent training rounds), and *policy initialisation* (i.e., the strategy for initialising the policy at the start of each fine-tuning cycle).

Our key contributions can be summarised as:

- We present the first formal investigation of overoptimisation dynamics across multiple RLHF iterations, relaxing assumptions made in previous work.

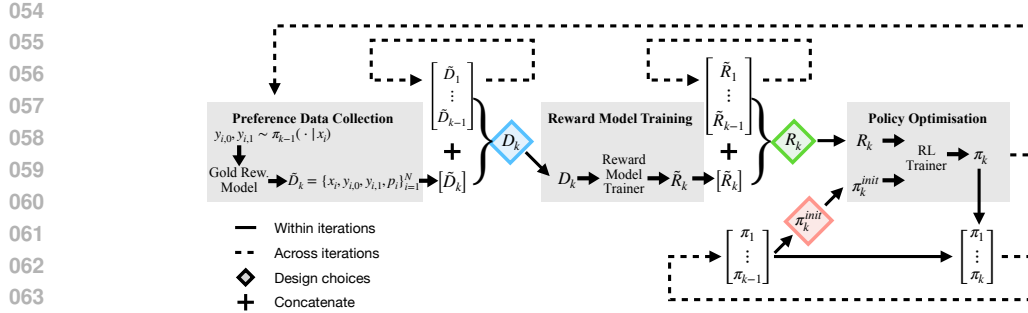


Figure 1: The Iterated RLHF framework performs multiple rounds of preference data collection, reward modelling, and policy optimisation. Our research reveals three design choices that dramatically impact performance: (1) how preference data is managed across iterations, (2) which reward function formulation to optimise, and (3) how policies are initialised at each stage. Effectively configuring these elements can significantly reduce overoptimisation.

- We discuss a systematic evaluation of key design choices with quantitative evidence of their impact on performance and overoptimisation.
- We provide practical guidelines for implementing iterated RLHF, including specific recommendations for preference data management, reward function selection, and policy initialisation strategies.

Using a gold-standard reward model to simulate human labellers (Coste et al., 2024; Gao et al., 2023) on the AlpacaFarm dataset (Taori et al., 2023) and working exclusively with open-source models, our experiments yield several key insights: Reward models become increasingly robust across iterations, leading to higher gold reward scores (Figure 2). Performance gains diminish after three iterations for most methods. Concatenating preference data across iterations dramatically outperforms other approaches. Small but persistent overoptimisation remains after four iterations regardless of design choices.

Our results demonstrate that while iterated RLHF significantly improves reward model robustness, it does not fully eliminate overoptimisation. This underscores the need for continued research into more robust alignment methods that can withstand sophisticated specification gaming (Krakovna et al., 2020) by increasingly capable language models.

2 RELATED WORK

RLHF is the standard for aligning large language models to human preference data. The iterated approach has been first discussed by Bai et al. (2022) to fix robustness and calibration issues, attributed to lack of data in the high score regime and has since gained in popularity (Ramé et al., 2024a; Xiong et al., 2024; Ye et al., 2024; Adolphs et al., 2023; Dong et al., 2024; Yuan et al., 2024). Besides training on newly collected preferences, an iterated scheme to train reward models from synthetically generated preference data has been proposed by Wang et al. (2024) and shown to improve performance on the reward model benchmark RewardBench (Lambert et al., 2024), but the authors focus on iterated training of an evaluator and do not study overoptimisation nor the design choices we consider. In the context of Direct Preference Optimisation (DPO) (Rafailov et al., 2023) offline, online and hybrid approaches repeatedly collecting new preference data have been investigated mostly in terms of sample efficiency (Xiong et al., 2024; Das et al., 2024; Muldrew

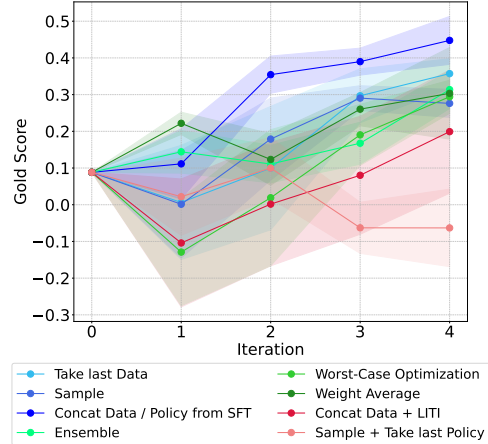


Figure 2: Iterated RLHF design choices in preference data management, reward function formulation, and policy initialization strongly affect ground truth performance and overoptimisation.

et al., 2024; Mehta et al., 2023). More broadly iterated methods have been investigated for machine teaching (Liu et al., 2017) and to resolve feedback loops caused by model deployment in supervised learning (Perdomo et al., 2020) and also performative RL (Mandal et al., 2023).

Overoptimisation is a common issue in RL, and evidence of this has been frequently reported in the RLHF literature (Ziegler et al., 2020; Stiennon et al., 2020; Gao et al., 2023; Singhal et al., 2024). A promising method to mitigate overoptimisation is using reward model ensembles combined with conservative optimisation (Coste et al., 2024). Several works further explore reward model ensembles in RLHF (Eisenstein et al., 2024; Lou et al., 2024). Notably, Ramé et al. (2024b) introduce weight averaged reward models (WARM) alleviating the inference cost of multiple reward models during training. Following Coste et al. (2024) and Gao et al. (2023) in tackling reward model overoptimisation, several works propose alternative approaches including reward model distillation (Fisch et al., 2024), hidden state regularisation (Yang et al., 2024b), and more (Yang et al., 2024a; Miao et al., 2024; Liu et al., 2024; Gorbatovski et al., 2024). One commonly reported mode of overoptimisation is length bias (Singhal et al., 2024; Park et al., 2024), which can be tackled by disentangling reward signals related to response length from content quality (Chen et al., 2024). To the best of our knowledge, the literature lacks a systematic investigation into overoptimisation in iterated Reinforcement Learning from Human Feedback (RLHF). Such an investigation is not only necessary but also fundamentally important for a deeper understanding and meaningful improvement of fine-tuning methods based on this technique.

3 ITERATED REINFORCEMENT LEARNING FROM HUMAN FEEDBACK

In this section, we first outline the process of a single iteration of RLHF and then extend it to the iterated framework. The RLH pipeline consists of the following three steps: 1. Collection of a preference dataset; 2. Reward model training; 3. Policy optimisation on the reward model. Though not an integral part of the RLHF pipeline, it is common in practice for step 1 to be preceded by supervised fine-tuning on labelled examples. To strengthen our investigation we developed a supporting theoretical framework based on performative prediction (Perdomo et al., 2020) that is presented in Appendix A.

3.1 SINGLE-ITERATION RLHF

Preference data collection. We start from a supervised fine-tuned policy π^{sft} (a policy checkpoint) and use it to collect preference data. The dataset \mathcal{D} contains tuples $\{x_i, y_{i,0}, y_{i,1}, p_i\}$ for $i = 1, \dots, N$, where $x_i \in \mathcal{X}$ is a prompt, $y_{i,j} \sim \pi^{sft}(\cdot|x_i)$ for $j = 0, 1$ are two responses from π^{sft} , and p_i indicates whether $y_{i,0}$ is preferred over $y_{i,1}$. Following Coste et al. (2024) and Gao et al. (2023), preferences p_i are simulated using a gold reward model R^* , which is significantly larger in terms of parameter size than the proxy reward models, serving as approximation for human labels in RLHF. **This use of the gold reward model is the standard approach for investigating overoptimisation without incurring significant costs and time bottlenecks due to human labelling. In Appendix E we conduct additional experiments with 25% label noise in the preference data.**

Reward model training. The proxy reward model R_ϕ is initialised from model checkpoint R^{init} , with a randomly initialised prediction head, and subsequently trained by minimizing the cross-entropy loss on the preference dataset \mathcal{D} . It is standard to use the Bradley-Terry model (Bradley & Terry, 1952), under which the probability of preferring the answer y_0 over y_1 given prompt x is given by

$$\mathbb{P}(y_0 \succ y_1|x) = \frac{1}{1 + \exp(R(x, y_1) - R(x, y_0))}. \quad (1)$$

Policy optimisation. Having trained the proxy reward model R_ϕ , the policy π_θ is initialised from π^{sft} and then fine-tuned to optimise R_ϕ . This is commonly achieved with the proximal policy optimization (PPO) algorithm (Schulman et al., 2017). In order to prevent overoptimisation of the proxy reward model and regularise π_θ to not diverge too drastically from its initialisation, a Kullback-Leibler divergence (KL) penalty is used. This yields the overall reward maximised as

$$R^{\text{PPO}}(x, y) = R_\phi(x, y) - \beta \log \left[\frac{\pi_\theta(y|x)}{\pi^{sft}(y|x)} \right], \quad (2)$$

where β controls the strength of the KL penalty (unless specified otherwise we set $\beta = 1 \times 10^{-4}$). This procedure, which only collects preferences once in the entire pipeline, has an important disadvantage. Reward models have been found to be poorly calibrated in the higher reward regime (Bai et al., 2022)

162
163
164**Algorithm 1** Iterated RLHF (design choices highlighted)

```

1: Inputs: Prompt dataset  $X = \{x_i\}_{i=1}^N$ ,  $\pi^{sft}$ ,  $R^{init}$ ,  $R^*$ , # of iterations  $n_{iter}$ 
2:  $\pi_0 \leftarrow \pi^{sft}$ 
3: for  $k = 1$  to  $n_{iter}$  do
4:    $y_{i,0}, y_{i,1} \sim \pi_{k-1}(x_i) \forall x_i \in X$ 
5:    $p_i \leftarrow R^*(x_i, y_{i,0}, y_{i,1}) \forall x_i \in D$ 
6:    $\tilde{\mathcal{D}}_k \leftarrow \{x_i, y_{i,0}, y_{i,1}, p_i\}_{i=1}^N$ 
7:    $\mathcal{D}_k \leftarrow \text{CombineData}([\tilde{\mathcal{D}}_1, \dots, \tilde{\mathcal{D}}_k])$ 
8:    $\tilde{R}_k \leftarrow \text{TrainRM}(R^{init}, \mathcal{D}_k)$ 
9:    $R_k \leftarrow \text{CombineRM}([\tilde{R}_1, \dots, \tilde{R}_k])$ 
10:   $\pi_k^{init} \leftarrow \text{CombineII}([\pi_0, \dots, \pi_{k-1}])$ 
11:   $\pi_k \leftarrow \text{TrainRL}(\pi_k^{init}, R_k)$ 
12: end for
13: return  $\pi_k$ 

```

and trained policies overoptimise the proxy reward model leading to unstable fine-tuned policies (Rafailov et al., 2024; Gao et al., 2023; Ziegler et al., 2020). Notably, policy optimization induces a divergence between the distributions $\pi_\theta(y|x)$ and $\pi^{sft}(y|x)$. This causes the optimised policy to generate outputs that are different from those seen in the training data \mathcal{D} . As a result, the reward model R_ϕ , which was trained on the data \mathcal{D} , is now being evaluated on data that it has not seen before.

3.2 ITERATED RLHF AND DESIGN CHOICES

The problem of the divergence between the distributions $\pi_\theta(y|x)$ and $\pi^{sft}(y|x)$ is the one addressed by iterated RLHF. In this process, multiple iterations of steps 1-3 of the RLHF pipeline (namely, collection of preference data, reward model training, and policy optimisation) are repeated as shown in Figure 1. Just as in the single-iteration setting, we start from the checkpoint π^{sft} and initialise the reward model from R^{init} with a randomly initialised prediction head. However, there are multiple design choices to be made when choosing how exactly to perform iterated RLHF training. We now describe the process in more detail, highlighting the design choices throughout. Please refer to Algorithm 1 for a schematic of the entire process. For simplicity of notation, we omit explicit references to the policy and reward model parameters θ and ϕ , using the subscript k to index iterations instead. During the k^{th} iteration of RLHF, we use the policy from the previous one, denoted by π_{k-1} to synthesise pairs of responses for the new preference data denoted by $\tilde{\mathcal{D}}_k$.

Indeed, using all policies is unnecessary as it equates to reapplying preference data, but at a higher cost. This new data enables the training of a proxy reward model for which the current policy's output is in-distribution, potentially mitigating the issue of overoptimisation. Taking into account previous iterations, we have access to the list of preference data $[\tilde{\mathcal{D}}_1, \dots, \tilde{\mathcal{D}}_k]$. Here we face the first design choice:

How do we combine the list of k preference datasets into a single training dataset \mathcal{D}_k ?

Combining preference data. Given a list of k preference datasets, the responses in each of which have been generated by different policies π_1, \dots, π_{k-1} , we identify three possible options to consolidate them into a single training dataset. The first option (Figure 3.a) is to simply set $\mathcal{D}_k = \tilde{\mathcal{D}}_k$, only training the reward model on the preference data collected in the current iteration. The second option at the other extreme (i.e., no inter-iteration transfer) is to concatenate all datasets (Figure 3.b). Reusing all the data at each iteration is expected to result in decreased overoptimisation and better approximation with respect to the true reward function. However, this comes with a reward model training computational cost that scales linearly with the number of iterations. Finally, balancing training time and information transfer, we keep the size of the reward model training data constant

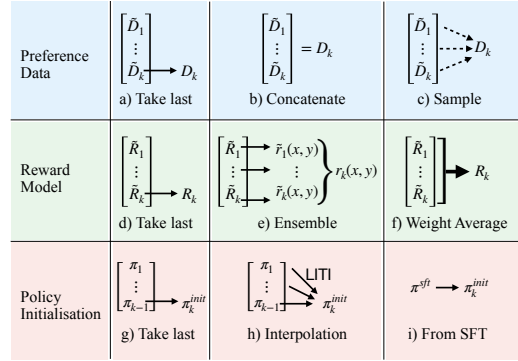


Figure 3: Design choices for Iterated RLHF (Algorithm 1). Options include how to combine preference data (latest only, concat, or sample), transfer reward models (last, ensemble, or weight averaged), and initialize policies (last, interpolate, or from SFT). These choices determine how learning signals are propagated through each iteration.

216 across iterations by sampling a subsets $\tilde{\mathcal{D}}_i$ for $i = 1, \dots, k$ and concatenating the subsets to form
 217 \mathcal{D}_k (Figure 3.c). Once the training data \mathcal{D}_k has been obtained, the proxy reward model \tilde{R}_k can be
 218 trained on it. \tilde{R}_k is initialised from the same base model in all iterations. Having trained the reward
 219 model, we now arrive at the second critical design choice:
 220

221 *How do we transfer information from the list of all previously trained proxy reward models
 222 $[\tilde{R}_1, \dots, \tilde{R}_k]$ into a single reward function R_k that can be optimised by the policy?*

223 **Combining reward models.** The reward model is the crucial piece in obtaining generalisable
 224 and consistent policies in RLHF, and it is even more important over multiple iterations as effects
 225 compound. Given the list $[\tilde{R}_1, \dots, \tilde{R}_k]$ containing the k proxy reward models leading up to the current
 226 iteration the task is to obtain a robust reward function to be optimised. We note that this design
 227 choice can be considered in parallel to the combination of preference data, as both target the same
 228 outcome of transferring information from previous iterations to the reward function.
 229

230 To achieve this task we investigate three types of solutions. The first only uses the most recently
 231 trained proxy reward model setting $R_k = \tilde{R}_k$ (Figure 3.d), hence there is no utilisation of previously
 232 trained reward models. In contrast, the second option ensembles all previously trained proxy
 233 RMs taking the mean of the individual rewards (Figure 3.e) (Coste et al., 2024). Since reward
 234 model ensembles showed limited improvements in Coste et al. (2024) we also evaluate worst-case
 235 optimisation (WCO), i.e., optimising the minimum $R_k(x, y) = \min_{i=1, \dots, k} \tilde{R}_i(x, y)$. This option
 236 comes with the disadvantage of requiring inference on k reward models in parallel. To address
 237 the computational cost, we also consider weight averaged reward models (see Figure 3.f) by
 238 performing task arithmetic (Ilharco et al., 2023). More formally, given a sequence of reward models
 239 $\tilde{R}_1, \dots, \tilde{R}_k$, which are parameterised by ϕ_1, \dots, ϕ_k , respectively, we obtain the proxy reward function
 240 R_k parameterised by ϕ_k as follows: The ensemble uses $R_k(x, y) = \frac{\sum_{i=1}^k \tilde{R}_i(x, y)}{k}$ and to obtain the
 241 weight averaged reward model we set $\phi_k = \frac{\sum_{i=1}^k \tilde{\phi}_i}{k}$. Having obtained the reward function, the next
 242 and final step of each iteration is to optimise it, which leads us to the third and final design choice:
 243

244 *Given π^{sft} and the fine-tuned policies π_1, \dots, π_{k-1} , how can we choose π_k^{init} to balance efficiency
 245 and robustness against overoptimisation?*

246 **Policy initialisation.** The final design choice concerns the initialisation of the policy, i.e., how
 247 π_k^{init} is chosen. Bai et al. (2022) initialise the policy from π^{sft} at every iteration, not taking into
 248 consideration previously performed computation. We call this initialisation *From SFT* shown in
 249 Figure 3.i. As alternative, we use linear interpolation towards initialisation (*LITI*) (Ramé et al.,
 250 2024a), which was inspired by WiSE-FT proposed by (Wortsman et al., 2022). With *LITI*, shown
 251 in Figure 3.h, we set $\pi_k^{init} = (1 - \eta)\pi_{k-1}^{init} + \eta\pi_{k-1}$, where η is a hyperparameter balances the
 252 optimisation of R_{k-1} . Taking $\eta = 1$ corresponds to initialising the current policy from the previously
 253 fine-tuned one, setting $\pi_k^{init} = \pi_{k-1}$. Since continuing fine-tuning of the most recent policy fully
 254 relies on the previous iterations, it may suffer from entropy collapse leading to no optimisation in
 255 later iterations. Continuing with the fine-tuned policy carries risks if undesirable behaviour learned
 256 in previous iterations cannot be unlearned. Note, when performing *LITI*, the policy is regularised
 257 with the KL between the policy and its initialisation π_k^{init} .
 258

4 EVALUATING OVEROPTIMISATION IN ITERATED RLHF

260 In Section 3 we formalised the process of iterated RLHF and highlighted the critical design choices.
 261 In this section, we detail our evaluation setup, emphasizing the quantification of overoptimisation
 262 and examining how its progression over iterations is influenced by different design choices.
 263

264 **Training setup.** Our evaluation setup follows extensive prior works that study overoptimisation in
 265 the single iteration RLHF in a controlled and simulated manner (Coste et al., 2024; Gao et al., 2023).
 266 Similarly to Coste et al. (2024) we use instructions from the *AlpacaFarm* dataset (Dubois et al., 2023)
 267 for reward model training and policy optimisation. The preference data $\tilde{\mathcal{D}}_k$ collected at each iteration
 268 contains preferences for a subset of 1000 instructions in the preference split of AlpacaFarm. Prefer-
 269 ence labels p_i are simulated with the 7 billion parameter Reward-Model-AlpacaFarm-Human
 270 (Dubois et al., 2023), which is also used by Coste et al. (2024). It is worth noting again the
 271 significant difference in parameter sizes between the proxy reward models and the gold reward
 272

270 model, justifying the use of the gold reward model as a proxy for human labellers. Similarly to Coste
 271 et al. (2024), to obtain π^{sft} , we performed supervised fine-tuning on the `pythia-410m` model
 272 (Biderman et al., 2023) on the AlpacaFarm SFT split. We chose `pythia-410m` as it achieves an
 273 appropriate balance between computational cost and experimental rigour for our investigation. Gao
 274 et al. (2023) also found that policy size did not affect the shape of the overoptimisation curve in
 275 their setting, further justifying this choice of policy. We initialise proxy reward models \tilde{R}_k from the
 276 HuggingFace checkpoint `pythia-70m_sft` provided by Coste et al. (2024), as well as the larger
 277 `pythia-160m`, with a randomly initialised prediction head (Coste et al., 2024). We train reward
 278 models for 5 epochs with a learning rate of 1×10^{-5} (Coste et al., 2024). For policy optimisation, we
 279 perform 6000 steps of PPO on the unlabelled split of AlpacaFarm. The learning rate is set to 1×10^{-6}
 280 and a constant KL penalty of 1×10^{-4} is used. The full specifications of the hyperparameters for
 281 reward model training and policy optimisation, and the prompt format are given in Appendix C.
 282

283 We perform a total of 4 iterations per method and report the results of the final iteration in comparison
 284 to the initial one. All results presented in our performance evaluation are reported for 8 random
 285 seeds, except for policy initialisation *From SFT* with the *Take last* configuration for both preference
 286 data and reward model, for which we only obtained 4 random seeds due to compute constraints. We
 287 note that this is still above the commonly reported 3 random seeds. To aggregate seeds in both gold
 288 score and KL we collect all seeds per iteration, bucket data points by KL. We then plot the mean
 289 and standard deviation of the gold rewards per bucket against the KL.

290 **Measuring overoptimisation with the Maximum Mean Discrepancy.** The standard methodology
 291 for investigating reward model overoptimisation is to compare mean rewards on proxy vs. gold reward
 292 functions over a hold-out set (Coste et al., 2024; Moskovitz et al., 2024; Gao et al., 2023). This over-
 293 looks discrepancies in the high-reward tail, which more strongly influence policy optimisation. We in-
 294 stead compare reward models by their distributions of rewards, evaluating on the 2000 unseen instruc-
 295 tions contained in the validation split of AlpacaFarm at every 300 steps during policy optimisation.
 296

297 Our approach to measuring differences between reward functions consists of two steps, the first of
 298 which is a standardisation that ensures reward functions that lead to the same ordering of policies
 299 when optimised are treated as equal (see Appendix B.1). In the second step, we use the maximum
 300 mean discrepancy (MMD) (Gretton et al., 2012) to measure the discrepancy between the two reward
 301 functions. In particular, we utilise this method to compare the proxy reward models trained at each
 302 iteration with the gold-reward model R^* . For full details and a justification of the validity of this
 303 method we refer the reader to Appendix B.

304 5 EXPERIMENTAL RESULTS

305 When comparing different methods, we primarily focus on their performance in the final iteration, as
 306 this iteration consistently outperforms previous ones for all algorithms. Additionally, it demonstrates
 307 the reward-KL curves produced by each method. We also compare the performance of methods
 308 across multiple iterations, to see how the KL-reward curves change through the iterations.

309 5.1 ITERATED RLHF CAN CLOSE THE GAP BETWEEN PROXY AND GOLD REWARD FUNCTIONS

310 Before investigating the differences between the design choices, we focus on the progression of
 311 reward model robustness across iterations more generally. In Figure 4, we show how performing
 312 multiple iterations of RLHF, concatenating all preference data to train the reward model, and re-
 313 initialising the policy from π^{sft} at each iteration decreases the gap between the gold reward function
 314 and the proxy. As iterations progress, the proxy reward model becomes more robust and increasingly
 315 aligned with the gold reward model on the distribution observed during policy optimisation.

316 Furthermore, the KL-reward Pareto front advances with each iteration, although improvements
 317 plateau as the distance between proxy and gold reward curves shrinks in later iterations. These
 318 performance plateaus appear to result from a combination of interacting factors rather than simple
 319 diminishing returns. First, the proxy reward model progressively converges toward the gold reward
 320 model on the distribution induced by policy optimisation, which limits the scope for further im-
 321 provement. Second, policy entropy tends to decline across iterations, particularly when initialisation
 322 methods other than *From SFT* are used. Third, data saturation may occur once additional preference
 323 data provides little novel information. However, there remains scope to better align gold and proxy
 324 reward functions. Comparing reward distributions across iterations further reveals that, after the

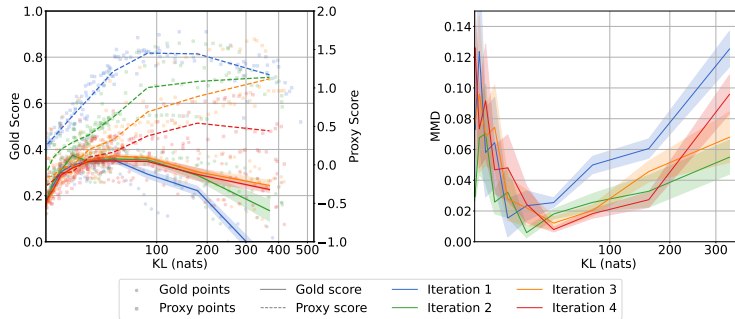


Figure 4: Progression of proxy–gold alignment across RLHF iterations with π^{sft} reinitialisation and concatenated data. Mean scores show narrowing gaps and improved robustness, though with diminishing returns. MMD reveals early convergence but rising divergence at higher KL, highlighting distributional shifts not observed in mean scores.

policy closely approximates the output distribution in \mathcal{D}_k , the MMD increases again in the high-KL regime for all iterations, especially rapidly in the initial iteration (see Figure 4). We hypothesize that the non-monotonic relationship between MMD and KL reflects a dynamic interplay between alignment and exploitation during training. Early on, RL against the proxy RM improves alignment with held-out samples from initialisation, reducing MMD as the proxy’s predictions grow closer to the gold RM. Later, as the policy distribution shifts and begins exploiting proxy-specific quirks (increasing KL), outputs diverge from true human preferences, driving MMD back up. Additionally, the rate at which the proxy-gold reward gap closes varies considerably among methods (see Appendix F.1), highlighting the importance of investigating design choices described in Section 3.

5.2 COMBINING PREFERENCE DATA

Scaling reward model training data is most effective. We first focus on comparing methods for combining preference datasets. To isolate the effects of varying the combination strategy, we fix the policy initialization to *From SFT* and reward models are combined using the *Take last* approach. As shown in Figure 5a, all methods demonstrate significant improvements over a single iteration, particularly in preventing performance collapse at higher KL divergences.

The *Concatenate* strategy achieves consistently higher gold scores, especially in the KL range of 50–200 nats. While *Take last* and *Sample* approaches show similar trends and substantial improvements over iteration 1, they do not quite match the performance of full data concatenation. This result is coherent with the finding that increasing training dataset size reduces reward model overoptimisation (Gao et al., 2023), explaining why the sampling strategy is outperformed by concatenating all datasets. A critical observation is that beyond $\text{KL} \approx 200$, the baseline iteration 1 experiences severe performance degradation due to overoptimisation, dropping to negative gold scores. In contrast, all iterative approaches maintain positive performance even at high KL values, demonstrating their effectiveness in mitigating overoptimisation. This ranking of methods is not only observed in the final iteration, but is already exhibited as early as the second iteration as shown in Figure 2 and in Appendix F.2.

Ensuring full coverage of the prompts when sampling matters less. While the sampling strategy slightly outperformed taking only the newest preference dataset, it did not achieve the same level of performance as concatenating all data. Here we take a closer look at the sampling strategy. In Figure 5b standard sampling with potential prompt repetition (*Sample*) and sampling where each prompt appears exactly once (*Sample Exclusive*). The differences are minor, suggesting that prompt repetition has a limited impact on performance or overoptimisation. This pattern also holds in earlier iterations (Appendix F.2), highlighting that while data combination strategies are effective at preventing overoptimisation, the computational cost of maintaining and training on growing datasets remains, as more efficient methods are unable to achieve the same performance as *Concatenate*. This motivates exploring reward-model combination in parameter space to achieve similar gains with less overhead.

5.3 COMBINING REWARD MODELS

No free lunch by merging reward models. Concatenating all preference data, previously the most effective method, serves as our performance baseline. As shown in Figure 5c, all approaches

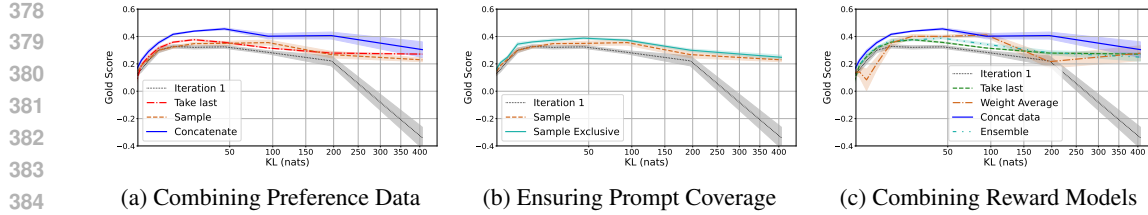


Figure 5: Iterated RLHF benefits most from scaling reward model training data. (a) Concatenating all preference data across iterations best mitigates overoptimisation, especially at mid KL (50–200). (b) Sampling, with or without prompt repetition, performs similarly, implying limited impact of prompt coverage. (c) Parameter-space methods (ensembles, averaging) lead to efficiency gains but fall short of the simpler *Take last* with data aggregation.

improve similarly in early KL regions (up to ≈ 50 nats), reaching comparable performance. *Weight Average* and *Ensemble* maintain strong, efficient performance, though ensembles increase inference time and memory use. The mean objective offers no clear gains over the *Take Last* approach with a single reward model, consistent with Coste et al. (2024). More specifically, Figure 5c shows that *Ensembling* does not outperform at the 70M scale. Although we do not explicitly measure calibration, MMD serves as a proxy for calibration in the high-reward tail, suggesting that either the calibration benefits are limited at this scale, or the optimisation with PPO exploits it regardless of calibration. While weight averaging has been reported to outperform ensembles (Ramé et al., 2024b), we only observe differences in the mid-KL regime. In contrast to prior work (Coste et al., 2024; Ramé et al., 2024b), we combine models trained on data with significantly different joint distribution over pairs (x, y) . Regardless, both methods still provide significant improvements when comparing the fourth and first iterations. The various reward model combination methods in RLHF perform similarly, suggesting computational efficiency should drive selection.

Larger reward models benefit more from combining reward models. We now investigate how scaling the reward model size affects performance in iterative RLHF. While concatenating all preference data with policy initialisation from the SFT checkpoint remains the most robust approach, we observe that alternative reward model strategies benefit significantly from increased reward model capacity. As shown in Figure 6, performance differences between the 70M and 160M reward models are most pronounced for *Ensemble* and *Worst-Case Optimisation*, with both methods substantially improving at the larger scale and approaching the performance of the data concatenation baseline by the fourth iteration. This suggests that while reward model combination methods did not match the effectiveness of preference data concatenation at smaller scales, their potential is unlocked with more expressive reward models. These results highlight that design choices affecting reward model size not only influence individual model accuracy but can significantly enhance the utility of design choices combining reward models in iterated RLHF settings.

5.4 POLICY INITIALISATION

Initialising from SFT is the most robust. Finally, comparing the policy initialisation methods we observe that no method improves on the KL-reward Pareto front achieved by concatenating all preference data and initialising the policy from the SFT checkpoint (Figure 7a). Sampling the preference data is similarly robust, highlighting that initialising with *From SFT* results in generally reduced overoptimisation. Note, *LITI* and *Take last* start from significantly larger KL due the compounding of KL through repeated initialisation increasingly further away from π^{sft} in the KL space. Resetting the policy at each iteration combined with the aggregation of preference data results

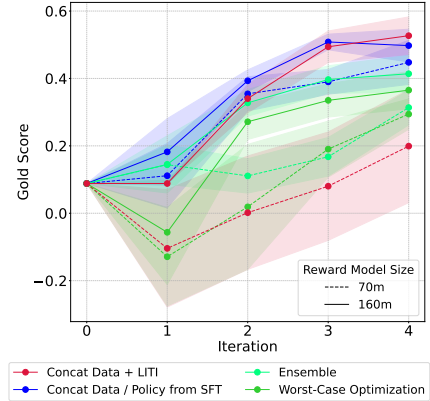


Figure 6: Impact of reward model size on gold score. Larger models (160M, solid) outperform smaller ones (70M, dashed), with the biggest gains in *Ensemble* and *Worst-Case Optimisation*. *From SFT* stays stable, while *LITI* steadily improves with scale.

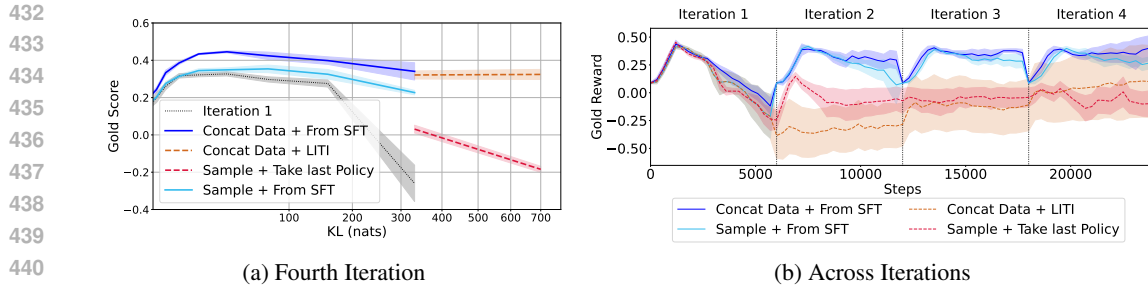


Figure 7: Effect of policy initialisation on overoptimisation and recovery across iterations. *From SFT* is most robust, avoiding divergence via resets and data aggregation. *LITI* and *Take last* start from high KL due to cumulative divergence. Overoptimised policies are hard to recover: *Take last* worsens over time, while *LITI* improves but does not reach *From SFT*.

in consistently less overoptimisation and more performant policies. Although, initialisation with π^{sft} limits the flexibility and potential gains that could be realised by continued optimisation.

Overoptimised policies are hard to recover from. While *From SFT* is reset at the end of each iteration, *LITI* and *Take last* have to recover from the initial overoptimisation, as shown in Figure 7b. The behaviour in earlier iterations reveals the consistent performance improvements attained with *LITI*. On the other hand, *Take last* is unable to recover after overoptimising again in the second iteration, despite the counterpart, sampling preference data but initialising *From SFT*, improving with each iteration. This is partly due to decreasing entropy caused by the prolonged optimisation when using the *Take last* initialisation (see Appendix F.5), the mean gold reward does not exceed zero in the third and fourth iterations. **However, the primary failure mode is the policy exploiting weaknesses and idiosyncrasies of the proxy reward models that cannot be corrected in following iterations.** In Appendix G we show an example of this behaviour, in which the response consists of narrow, repeated token sequences. Despite *LITI* improving on average across multiple seeds, we observe that linear interpolation is also unable to recover strongly overoptimised seeds (see Appendix F.4). Thus, while *From SFT* is most robust, it is also limited by the repeated initialisation from π^{sft} .

Policy interpolation works better with larger reward models. We hypothesise that *LITI* could achieve similar or higher gold scores than *From SFT* after more iterations. Supporting this, our experiments with a larger reward model show that *LITI* benefits substantially from increased reward model capacity (see Figure 6). This improvement likely stems both from better-calibrated gradients that support recovery, and from the fact that larger reward models tend to overoptimise less aggressively (Gao et al., 2023), resulting in safer intermediate policies and more stable interpolation paths. These findings highlight the importance of early stopping and reward model design when using policy initialisation methods other than *From SFT*, and suggest that *LITI* may become increasingly competitive as reward model expressiveness scales. **Despite promising scaling results of *LITI*, *From SFT* initialisation remains the safe option for less expressive reward models.**

5.5 REWARD MODEL EVALUATION ON REWARDBENCH

We evaluate the reward models from the first and final iterations obtained via the different design choices on RewardBench (Lambert et al., 2024). In particular, since we train on AlpacaFarm, we report the performance on the AlpacaEval Easy and Hard splits as well as the overall accuracy averaged across all subsets of the benchmark.

In Figure 8 we observe that the proxy reward models, which correspond to methods that ultimately achieve high gold reward in the final iteration, obtain higher or comparable accuracy on the AlpacaEval subsets when comparing the first and final iterations. For the larger reward models, this is the case for *Concat Data* as well as for *LITI*. The remaining design choices yield final reward models that achieve lower accuracy on AlpacaEval subsets than their counterparts trained in the initial iteration. The full results, also including the 70M reward models, can be found in Appendix D.

While this evaluation on RewardBench provides an additional perspective on the generalization of the proxy reward models, we note that RewardBench performance is less diagnostic for our setting than gold-reward alignment. Due to distribution shift, reward models in later iterations may effectively mitigate overoptimisation even if their accuracy on the RewardBench test set is lower.

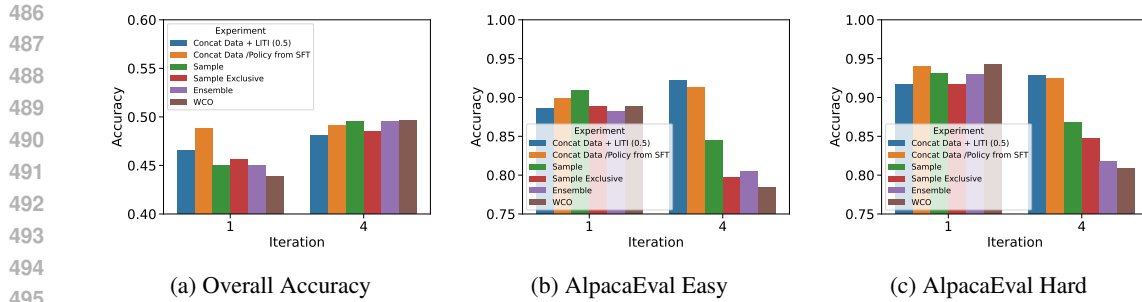


Figure 8: RewardBench performance for 160M reward models.

6 LIMITATIONS

Our study focuses on controlled settings, using modestly sized policy models (Pythia-410M) and reward models (70M, 160M) on the AlpacaFarm benchmark with a static “gold” reward model to simulate human feedback. However, this setup, consistent with prior work (Coste et al., 2024; Ramé et al., 2024b; Zhu et al., 2024) (also in terms of model size), enables systematic investigation of iterative RLHF while ensuring results remain interpretable and comparable. Moreover, scaling laws suggest policy size is not the main driver of overoptimisation and that scale effects are smooth (Gao et al., 2023), indicating that our findings and design choices are likely to transfer to larger models, even if the degree or speed of overoptimisation differs. Using a single dataset (AlpacaFarm) enabled controlled ablations but may not capture the diversity of real-world tasks. We also note that a static “gold” reward model, abstracts away the noisy and evolving nature of human preferences. However, this is standard practice in the field (Coste et al., 2024; Gao et al., 2023) to ensure reproducibility and mitigate cost of human labelling. [In Appendix E, we conduct experiments with simulated label noise, which show that our conclusions extend to this more realistic setting. Preference drift remains an interesting problem that is beyond the scope of this paper.](#) We ran four iterations, enough to observe plateaus and overoptimisation trends, but further scaling was prohibitive given the computational resources of our institution. Nonetheless, our work offers key insights and guidance for designing more robust iterative RLHF pipelines and lays groundwork for future research on larger scales and real-world settings.

7 CONCLUSION

In this work we have presented the first investigation of reward model overoptimisation in iterated RLHF. Through simulations with a gold-standard reward model and analysing distributional discrepancies, we have demonstrated that overoptimisation diminishes across iterations as reward models better approximate the ground truth. However, improvements begin to plateau after three iterations. [Consequently, we recommend prioritizing a smaller number of iterations with *Concat Data* rather than attempting to match performance by extending cheaper strategies such as *Take Last*, as the latter incurs a considerably higher overall cost. It is worth noting that larger reward models exhibit stronger performance when using *Ensemble* and *WCO* strategies.](#) While completely eliminating overoptimisation remains unattainable, we have identified base policy initialisation as the most robust approach, despite its reduced optimisation flexibility. Our analysis provides practical guidelines for implementing iterated RLHF and illuminates fundamental trade-offs in iterative preference learning, establishing a foundation for future research in reliable RLHF systems.

ETHICS STATEMENT

We have carefully considered the broader impact of this work. Our research focuses on overoptimisation in reinforcement learning from human feedback (RLHF), which is an important area for improving alignment between AI systems and human preferences. While RLHF as a field has potential implications for fairness, bias, and the societal impact of large-scale deployment, the contributions in this paper are methodological and do not involve sensitive data, human subjects, or direct deployment in real-world applications. We therefore do not anticipate any immediate ethical concerns arising directly from this work.

540 REPRODUCIBILITY STATEMENT
541

542 We have taken several steps to ensure the reproducibility of our work. All models and benchmarks
543 used in our study are open source, with appropriate links and licensing information provided. Detailed
544 descriptions of the training procedures are presented in Section 4, and the full set of hyperparameters
545 as well as the prompts used during training are reported in Appendix C. To account for variability,
546 all experiments are conducted across eight random seeds. We commit to releasing our code upon
547 acceptance of the paper to further facilitate reproducibility.

548
549 LLM USAGE STATEMENT
550

551 We used LLMs, in particular ChatGPT and Claude to aide the writing process. Specifically, for
552 paraphrasing and shortening existing paragraphs of the manuscript, as well as polishing the wording
553 of certain paragraphs for clarity.

554
555 REFERENCES
556

557 Leonard Adolphs, Tianyu Gao, Jing Xu, Kurt Shuster, Sainbayar Sukhbaatar, and Jason Weston. The
558 CRINGE loss: Learning what language not to model. In *Proceedings of the 61st Annual Meeting*
559 *of the Association for Computational Linguistics (ACL'23)*, 2023.

560 Yuntao Bai, Andy Jones, Kamal Ndousse, Amanda Askell, Anna Chen, Nova DasSarma, Dawn
561 Drain, Stanislav Fort, Deep Ganguli, Tom Henighan, Nicholas Joseph, Saurav Kadavath, Jackson
562 Kernion, Tom Conerly, Sheer El-Showk, Nelson Elhage, Zac Hatfield-Dodds, Danny Hernandez,
563 Tristan Hume, Scott Johnston, Shauna Kravec, Liane Lovitt, Neel Nanda, Catherine Olsson, Dario
564 Amodei, Tom Brown, Jack Clark, Sam McCandlish, Chris Olah, Ben Mann, and Jared Kaplan.
565 Training a helpful and harmless assistant with reinforcement learning from human feedback. *arXiv*
566 *preprint arXiv:2204.05862*, 2022.

567 Stella Biderman, Hailey Schoelkopf, Quentin Gregory Anthony, Herbie Bradley, Kyle O'Brien, Eric
568 Hallahan, Mohammad Aftab Khan, Shivanshu Purohit, USVSN Sai Prashanth, Edward Raff, et al.
569 Pythia: A suite for analyzing large language models across training and scaling. In *International*
570 *Conference on Machine Learning*, pp. 2397–2430. PMLR, 2023.

571 Ralph Allan Bradley and Milton E. Terry. Rank analysis of incomplete block designs: I. the method
572 of paired comparisons. *Biometrika*, 39(3/4):324–345, 1952.

573 Lichang Chen, Chen Zhu, Juhai Chen, Davit Soselia, Tianyi Zhou, Tom Goldstein, Heng Huang,
574 Mohammad Shoeybi, and Bryan Catanzaro. ODIN: Disentangled reward mitigates hacking in
575 RLHF. In *Proceedings of the 41st International Conference on Machine Learning (ICML'24)*,
576 2024.

577 Thomas Coste, Usman Anwar, Robert Kirk, and David Krueger. Reward model ensembles help
578 mitigate overoptimization. In *Proceedings of the 12th International Conference on Learning*
579 *Representations (ICLR'24)*, 2024.

581 Nirjhar Das, Souradip Chakraborty, Aldo Pacchiano, and Sayak Ray Chowdhury. Provably Sample
582 Efficient RLHF via Active Preference Optimization. *arXiv preprint arXiv:2402.10500*, 2024.

583 Hanze Dong, Wei Xiong, Bo Pang, Haoxiang Wang, Han Zhao, Yingbo Zhou, Nan Jiang, Doyen
584 Sahoo, Caiming Xiong, and Tong Zhang. RLHF Workflow: From Reward Modeling to Online
585 RLHF. *Transactions on Machine Learning Research*, September 2024.

587 Yann Dubois, Xuechen Li, Rohan Taori, Tianyi Zhang, Ishaan Gulrajani, Jimmy Ba, Carlos Guestrin,
588 Percy Liang, and Tatsunori B. Hashimoto. AlpacaFarm: A Simulation Framework for Methods
589 that Learn from Human Feedback. In *Proceedings of the 37th Annual Conference on Neural*
590 *Information Processing Systems (NeurIPS'23)*, 2023.

591 Jacob Eisenstein, Chirag Nagpal, Alekh Agarwal, Ahmad Beirami, Alex D'Amour, DJ Dvijotham,
592 Adam Fisch, Katherine Heller, Stephen Pföh, Deepak Ramachandran, et al. Helping or herding?
593 reward model ensembles mitigate but do not eliminate reward hacking. In *Proceedings of the 1st*
594 *Conference on Language Modeling (COLM'24)*, 2024.

594 Adam Fisch, Jacob Eisenstein, Vicky Zayats, Alekh Agarwal, Ahmad Beirami, Chirag Nagpal, Pete
 595 Shaw, and Jonathan Berant. Robust preference optimization through reward model distillation.
 596 *arXiv preprint arXiv:2405.19316*, 2024.

597 Leo Gao, John Schulman, and Jacob Hilton. Scaling Laws for Reward Model Overoptimization. In
 598 *Proceedings of the 40th International Conference on Machine Learning (ICML'23)*, 2023.

600 Adam Gleave, Michael Dennis, Cody Wild, Neel Kant, Sergey Levine, and Stuart Russell. Adversarial
 601 Policies: Attacking Deep Reinforcement Learning. In *Proceedings of the 8th International*
 602 *Conference on Learning Representations (ICLR'20)*, 2020.

603 Alexey Gorbatovski, Boris Shaposhnikov, Alexey Malakhov, Nikita Surnachev, Yaroslav Aksnov,
 604 Ian Maksimov, Nikita Balagansky, and Daniil Gavrilov. Learn your reference model for real good
 605 alignment. *arXiv preprint arXiv:2404.09656*, 2024.

607 Arthur Gretton, Karsten M. Borgwardt, Malte J. Rasch, Bernhard Schölkopf, and Alexander Smola.
 608 A kernel two-sample test. *Journal of Machine Learning Research*, 13(25):723–773, 2012.

609 Gabriel Ilharco, Marco Tulio Ribeiro, Mitchell Wortsman, Suchin Gururangan, Ludwig Schmidt,
 610 Hannaneh Hajishirzi, and Ali Farhadi. Editing models with task arithmetic. In *Proceedings of the*
 611 *11th International Conference on Learning Representations (ICLR'23)*, 2023.

612 Victoria Krakovna, Jonathan Uesato, Vladimir Mikulik, Matthew Rahtz, Tom Everitt,
 613 Ramana Kumar, Zac Kenton, Jan Leike, and Shane Legg. Specification gaming:
 614 the flip side of ai ingenuity. <https://deepmind.google/discover/blog/specification-gaming-the-flip-side-of-ai-ingenuity/>, 2020. Accessed:
 615 2025-05-02.

617 Andreas Köpf, Yannic Kilcher, Dimitri von Rütte, Sotiris Anagnostidis, Zhi-Rui Tam, Keith Stevens,
 618 Abdullah Barhoum, Nguyen Minh Duc, Oliver Stanley, Richárd Nagyfi, Shahul ES, Sameer
 619 Suri, David Glushkov, Arnav Dantuluri, Andrew Maguire, Christoph Schuhmann, Huu Nguyen,
 620 and Alexander Mattick. OpenAssistant Conversations – Democratizing Large Language Model
 621 Alignment. In *NeurIPS 2023 Datasets and Benchmarks*, 2023.

623 Nathan Lambert, Valentina Pyatkin, Jacob Morrison, LJ Miranda, Bill Yuchen Lin, Khyathi Chandu,
 624 Nouha Dziri, Sachin Kumar, Tom Zick, Yejin Choi, Noah A. Smith, and Hannaneh Hajishirzi. Re-
 625 wardBench: Evaluating Reward Models for Language Modeling. *arXiv preprint arXiv:2403.13787*,
 626 2024.

627 Weiyang Liu, Bo Dai, Ahmad Humayun, Charlene Tay, Chen Yu, Linda B. Smith, James M. Rehg,
 628 and Le Song. Iterative machine teaching. In Doina Precup and Yee Whye Teh (eds.), *Proceedings*
 629 *of the 34th International Conference on Machine Learning*, volume 70 of *Proceedings of Machine*
 630 *Learning Research*, pp. 2149–2158, 06–11 Aug 2017.

631 Zhihan Liu, Miao Lu, Shenao Zhang, Boyi Liu, Hongyi Guo, Yingxiang Yang, Jose Blanchet, and
 632 Zhaoran Wang. Provably Mitigating Overoptimization in RLHF: Your SFT Loss is Implicitly an
 633 Adversarial Regularizer. In *Proceedings of the 38th Annual Conference on Neural Information*
 634 *Processing Systems (NeurIPS'24)*, 2024.

636 Xingzhou Lou, Dong Yan, Wei Shen, Yuzi Yan, Jian Xie, and Junge Zhang. Uncertainty-aware reward
 637 model: Teaching reward models to know what is unknown. *arXiv preprint arXiv:2410.00847*,
 638 2024.

639 Debmalya Mandal, Stelios Triantafyllou, and Goran Radanovic. Performative reinforcement learning.
 640 In *Proceedings of the 40th International Conference on Machine Learning*, ICML'23. JMLR.org,
 641 2023.

642 Viraj Mehta, Vikramjeet Das, Ojash Neopane, Yijia Dai, Ilija Bogunovic, Jeff Schneider, and
 643 Willie Neiswanger. Sample Efficient Reinforcement Learning from Human Feedback via Active
 644 Exploration. *arXiv preprint arXiv:2312.00267*, 2023.

646 Yuchun Miao, Sen Zhang, Liang Ding, Rong Bao, Lefei Zhang, and Dacheng Tao. InfoRM: Mitigating
 647 Reward Hacking in RLHF via Information-Theoretic Reward Modeling. In *Proceedings of the*
 648 *38th Annual Conference on Neural Information Processing Systems (NeurIPS'24)*, 2024.

648 Ted Moskovitz, Aaditya K. Singh, DJ Strouse, Tuomas Sandholm, Ruslan Salakhutdinov, Anca D.
 649 Dragan, and Stephen McAleer. Confronting Reward Model Overoptimization with Constrained
 650 RLHF. In *Proceedings of the 12th International Conference on Learning Representations*
 651 (*ICLR*'24), 2024.

652 William Muldrew, Peter Hayes, Mingtian Zhang, and David Barber. Active preference learning for
 653 large language models. In *Proceedings of the 41st International Conference on Machine Learning*
 654 (*ICML*'24), 2024.

655 Long Ouyang, Jeff Wu, Xu Jiang, Diogo Almeida, Carroll L. Wainwright, Pamela Mishkin, Chong
 656 Zhang, Sandhini Agarwal, Katarina Slama, Alex Ray, John Schulman, Jacob Hilton, Fraser Kelton,
 657 Luke Miller, Maddie Simens, Amanda Askell, Peter Welinder, Paul Christiano, Jan Leike, and
 658 Ryan Lowe. Training language models to follow instructions with human feedback. *arXiv preprint*
 659 *arXiv:2203.02155*, 2022.

660

661 Ryan Park, Rafael Raffailov, Stefano Ermon, and Chelsea Finn. Disentangling length from quality in
 662 direct preference optimization. In *Findings of the Association for Computational Linguistics: ACL*
 663 2024, pp. 4998–5017, 2024.

664

665 Juan Perdomo, Tijana Zrnic, Celestine Mendler-Dünner, and Moritz Hardt. Performative prediction.
 666 In *Proceedings of the 37th International Conference on Machine Learning* (*ICML*'20), 2020.

667

668 Rafael Raffailov, Archit Sharma, Eric Mitchell, Stefano Ermon, Christopher D. Manning, and Chelsea
 669 Finn. Direct Preference Optimization: Your Language Model is Secretly a Reward Model. In *Pro-
 670 ceedings of the 37th Annual Conference on Neural Information Processing Systems* (*NeurIPS*'23),
 671 2023.

672 Rafael Raffailov, Yaswanth Chittep, Ryan Park, Harshit Sikchi, Joey Hejna, W. Bradley Knox,
 673 Chelsea Finn, and Scott Niekum. Scaling laws for reward model overoptimization in direct
 674 alignment algorithms. In *Proceedings of the 38th Annual Conference on Neural Information
 675 Processing Systems* (*NeurIPS*'24), 2024.

676

677 Alexandre Ramé, Johan Ferret, Nino Vieillard, Robert Dadashi, Léonard Hussenot, Pierre-Louis
 678 Cedoz, Pier Giuseppe Sessa, Sertan Girgin, Arthur Douillard, and Olivier Bachem. WARP: On the
 679 Benefits of Weight Averaged Rewarded Policies. *arXiv preprint arXiv:2406.16768*, 2024a.

680

681 Alexandre Ramé, Nino Vieillard, Léonard Hussenot, Robert Dadashi, Geoffrey Cideron, Olivier
 682 Bachem, and Johan Ferret. WARM: On the Benefits of Weight Averaged Reward Models, 2024b.

683

684 John Schulman, Filip Wolski, Prafulla Dhariwal, Alec Radford, and Oleg Klimov. Proximal policy
 685 optimization algorithms. *arXiv preprint arXiv:1707.06347*, 2017.

686

687 Prasann Singhal, Tanya Goyal, Jiacheng Xu, and Greg Durrett. A Long Way to Go: Investigating
 688 Length Correlations in RLHF. In *Proceedings of the 1st Conference on Language Modeling*
 689 (*COLM*'24), 2024.

690

691 Joar Skalse, Lucy Farnik, Sumeet Ramesh Motwani, Erik Jenner, Adam Gleave, and Alessandro
 692 Abate. STARC: A General Framework For Quantifying Differences Between Reward Functions.
 693 In *Proceedings of the 12th International Conference on Machine Learning* (*ICML*'24), 2024.

694

695 Nisan Stiennon, Long Ouyang, Jeff Wu, Daniel M. Ziegler, Ryan Lowe, Chelsea Voss, Alec Radford,
 696 Dario Amodei, and Paul Christiano. Learning to summarize from human feedback. In *Proceedings*
 697 of the 34th Annual Conference on Neural Information Processing Systems (*NeurIPS*'20), 2020.

698

699 Rohan Taori, Ishaan Gulrajani, Tianyi Zhang, Yann Dubois, Xuechen Li, Carlos Guestrin, Percy
 700 Liang, and Tatsunori B. Hashimoto. Stanford Alpaca: An Instruction-following LLaMA model.
 701 https://github.com/tatsu-lab/stanford_alpaca, 2023.

702

703 Tianlu Wang, Ilia Kulikov, Olga Golovneva, Ping Yu, Weizhe Yuan, Jane Dwivedi-Yu,
 704 Richard Yuanzhe Pang, Maryam Fazel-Zarandi, Jason Weston, and Xian Li. Self-taught evaluators.
 705 *arXiv preprint arXiv:2408.02666*, 2024.

702 Mitchell Wortsman, Gabriel Ilharco, Jong Wook Kim, Mike Li, Simon Kornblith, Rebecca Roelofs,
 703 Raphael Gontijo Lopes, Hannaneh Hajishirzi, Ali Farhadi, Hongseok Namkoong, and Ludwig
 704 Schmidt. Robust fine-tuning of zero-shot models. In *Proceedings of the 2022 IEEE/CVF Confer-
 705 ence on Computer Vision and Pattern Recognition (CVPR'22)*, 2022.

706 Wei Xiong, Hanze Dong, Chenlu Ye, Ziqi Wang, Han Zhong, Heng Ji, Nan Jiang, and Tong Zhang.
 707 Iterative preference learning from human feedback: Bridging theory and practice for RLHF
 708 under KL-constraint. In *Proceedings of the 41st International Conference on Machine Learning
 709 (ICML'24)*, 2024.

710 Adam X. Yang, Maxime Robeyns, Thomas Coste, Jun Wang, Haitham Bou-Ammar, and Laurence
 711 Aitchison. Bayesian Reward Models for LLM Alignment. In *Proceedings of the ICLR 2024
 712 Workshop on Secure and Trustworthy Large Language Models*, 2024a.

713 Rui Yang, Ruomeng Ding, Yong Lin, Huan Zhang, and Tong Zhang. Regularizing Hidden States
 714 Enables Learning Generalizable Reward Model for LLMs. In *Proceedings of the 38th Annual
 715 Conference on Neural Information Processing Systems (NeurIPS'24)*, 2024b.

716 Chenlu Ye, Wei Xiong, Yuheng Zhang, Nan Jiang, and Tong Zhang. Online Iterative Reinforcement
 717 Learning from Human Feedback with General Preference Model. In *Proceedings of the 41st
 718 Annual Conference on Neural Information Processing Systems (NeurIPS'24)*, 2024.

719 Weizhe Yuan, Richard Yuanzhe Pang, Kyunghyun Cho, Xian Li, Sainbayar Sukhbaatar, Jing Xu,
 720 and Jason Weston. Self-rewarding language models. In *Proceedings of the 41st International
 721 Conference on Machine Learning (ICML'24)*, 2024.

722 Banghua Zhu, Michael I. Jordan, and Jiantao Jiao. Iterative Data Smoothing: Mitigating Reward
 723 Overfitting and Overoptimization in RLHF, 2024.

724 Daniel M. Ziegler, Nisan Stiennon, Jeffrey Wu, Tom B. Brown, Alec Radford, Dario Amodei, Paul
 725 Christiano, and Geoffrey Irving. Fine-tuning language models from human preferences. *arXiv
 726 preprint arXiv:1909.08593*, 2020.

727

728

729

730

731

732

733

734

735

736

737

738

739

740

741

742

743

744

745

746

747

748

749

750

751

752

753

754

755

756 **A A THEORETICAL FRAMEWORK: ITERATED RLHF AND PERFORMATIVE**
 757 **PREDICTION**
 758

759 **A.1 OVERVIEW**
 760

761 We note that the framework of performative prediction (Perdomo et al., 2020) can be applied to
 762 our setting. In fact, when performing iterated RLHF, we are simulating performative prediction or
 763 more specifically a version of strategic classification. We have that a reward model R_ϕ induces a
 764 potentially different distribution $\mathcal{D}(\phi)$ over instances (x, y) where continuations y are obtained from
 765 the policy π_θ optimised for R_ϕ , which yields that a reward model $R_{\phi_{PO}}$ is performatively optimal
 766 if $\phi_{PO} = \arg \min_{\phi} \mathbb{E}_{(x,y) \sim \mathcal{D}(\phi)} \ell((x, y, \phi))$. Furthermore, a model $R_{\phi_{PS}}$ is defined as performatively
 767 stable if $\phi_{PS} = \arg \min_{\phi} \mathbb{E}_{(x,y) \sim \mathcal{D}(\phi_{PS})} \ell((x, y, \phi))$. Intuitively, retraining a performatively stable
 768 reward model after optimising against it will yield the same reward model. As such the reward model
 769 would not be over-optimised and still perform optimally on its induced distribution. In Theorem 3.5
 770 Perdomo et al. (2020) provide 3 conditions under which the reward model obtained from repeated
 771 iterations of RLHF converges to a unique performatively stable reward model at a linear rate. We
 772 require the loss to be β -jointly smooth and γ -strongly convex, and the map $\mathcal{D}(\cdot)$ from reward model
 773 parameters to the distribution of prompt continuation pairs to be ϵ -sensitive. Since as part of the
 774 map $\mathcal{D}(\cdot)$ the policy is optimised with PPO, where small changes in the reward model can lead to
 775 significant changes in the optimal policy, this mapping is generally not ϵ -sensitive. As a consequence,
 776 linear convergence is not guaranteed. Note, that we may still aim for close to linear convergence by
 777 making adjustments to satisfy the stated conditions.
 778

779 In the following subsections we expand on the overview above and present a concise theoretical
 780 account of iterated RLHF. We use ϕ to denote reward-model parameters and θ to denote policy
 781 parameters. Our presentation casts iterated RLHF as a performative prediction problem, and then
 782 derives sufficient conditions for convergence as well as a set of practical propositions that explain
 783 common empirical mitigations (data aggregation, reward model ensembles, and policy resetting).
 784

785 **A.2 SETUP**
 786

787 Let π_θ be a stochastic policy parameterised by $\theta \in \Theta$. Let R_ϕ be a learned reward model parame-
 788 terised by $\phi \in \Phi$. We denote by $\Pi(R_\phi) \mapsto \pi_{\theta(\phi)}$ the policy optimisation operator that (approximately)
 789 returns a policy optimised with respect to R_ϕ . Running $\pi_{\theta(\phi)}$ in the environment (or simulator)
 790 induces a distribution over prompts and model responses; we write $D(\phi)$ for the resulting distribution
 791 over observed preference pairs or (*input, response*) tuples (x, y) .
 792

793 A reward model is trained by empirical risk minimization on data sampled from the distribution
 794 induced by the current reward model through policy optimisation. Concretely, given a loss function
 795 $\ell(\phi; (x, y))$ (for example cross-entropy or a surrogate for pairwise preference loss), the standard
 796 iterated update considered throughout this work can be defined as follows:
 797

$$\phi_{t+1} = \arg \min_{\phi} \mathbb{E}_{(x,y) \sim D(\phi_t)} [\ell(\phi; (x, y))]. \quad (3)$$

798 This framing matches the performative prediction viewpoint: the object being learned (the reward
 799 model) affects the data distribution through the downstream policy it induces.
 800

801 **A.3 PERFORMATIVE STABILITY**
 802

803 **Definition A.1** (Performative stability). A reward model parameter ϕ^* is called performatively stable
 804 if it is a fixed point of the update equation 3, i.e.
 805

$$\phi^* = \arg \min_{\phi} \mathbb{E}_{(x,y) \sim D(\phi^*)} [\ell(\phi; (x, y))].$$

806 At a performatively stable point, retraining the reward model on data produced by the policy it induces
 807 produces no change. Iterated RLHF can therefore be interpreted as an algorithmic attempt to reach
 808 such a fixed point.
 809

810 A.4 CONVERGENCE GUARANTEES
811

812 **Theorem A.2** (Convergence to a performatively stable point). *Suppose the per-example loss*
 813 *$\ell(\phi; (x, y))$ is α -strongly convex and β -smooth in ϕ for every data point (x, y) . Suppose further that*
 814 *the mapping $\phi \mapsto D(\phi)$ is L -Lipschitz in total variation distance. If $\frac{L\beta}{\alpha} < 1$, then the map defined*
 815 *by the update equation 3 is a contraction and the iterates $\{\phi_t\}_{t \geq 0}$ converge linearly to a unique*
 816 *performatively stable point ϕ^* .*

817 *Proof sketch.* For each fixed data distribution, strong convexity and smoothness imply the population
 818 risk admits a unique minimizer, and the $\arg \min$ mapping is Lipschitz with constant at most β/α . Composing this with the L -Lipschitz dependence of $D(\phi)$ on ϕ yields an overall contraction constant
 819 bounded by $L\beta/\alpha$. If this constant is strictly less than one, Banach's fixed point theorem guarantees
 820 a unique fixed point and geometric convergence of iterates. This is an application of the performatively
 821 prediction contraction framework (Perdomo et al., 2020).
 822

823 **Discussion.** The theorem isolates two failure modes in practice: (i) the loss used to train reward
 824 models is rarely globally strongly convex in modern neural parameterisations, and (ii) modern policy
 825 optimisers (PPO, SAC, etc.) can induce highly non-Lipschitz changes in the data distribution, i.e.,
 826 small changes to ϕ may yield large shifts in $\pi_{\theta(\phi)}$ and hence in $D(\phi)$. Consequently, the sufficient
 827 conditions above are not satisfied in general RLHF pipelines, but they nevertheless clarify why certain
 828 regularisers and protections (e.g., constraining policy updates, aggregating data) promote stable
 829 behaviour.
 830

831 A.5 PREFERENCE DATA AGGREGATION
832

833 **Proposition A.3** (Data aggregation reduces estimation error). *Let the reward model be trained by*
 834 *empirical risk minimization on a dataset \mathcal{S} of size N . Under standard i.i.d. concentration bounds, the*
 835 *expected generalization error of the empirical minimizer scales as $O(1/\sqrt{N})$. If datasets collected*
 836 *across iterations $\mathcal{S}_1, \dots, \mathcal{S}_T$ are concatenated to form \mathcal{S}_{tot} with total size $N_{\text{tot}} = \sum_{t=1}^T N_t$, the*
 837 *estimation error correspondingly decreases as $O(1/\sqrt{N_{\text{tot}}})$.*

838 *Proof sketch.* This follows from Hoeffding-type concentration or uniform convergence arguments:
 839 more samples tighten empirical estimates of the population risk and hence reduce the gap between
 840 empirical and population minima.
 841

842 **Corollary A.4.** *Training on aggregated data approximates training on the mixture distribution*
 843 *$D_{\text{mix}} = \frac{1}{T} \sum_{t=1}^T D(\phi_t)$, reducing variance and decreasing sensitivity to idiosyncrasies of any single*
 844 *iteration.*

845 **Discussion.** Aggregation stabilizes training in two ways: it increases effective sample size (reducing
 846 estimation noise) and smooths the effective data generating process, which can reduce the Lipschitz
 847 constant of $\phi \mapsto D(\phi)$ empirically.
 848

849 A.6 REWARD-MODEL ENSEMBLES AND TRANSFER
850

851 **Proposition A.5** (Averaging reduces squared error). *Let $R_{\phi_i} = R^* + \delta_i$ be K proxy reward models*
 852 *with additive errors δ_i . Let define the ensemble reward as: $R_{\text{ens}} = \frac{1}{K} \sum_{i=1}^K R_{\phi_i} = R^* + \frac{1}{K} \sum_{i=1}^K \delta_i$. Then*

$$856 |R_{\text{ens}} - R^*|_2^2 = \left| \frac{1}{K} \sum_{i=1}^K \delta_i \right|_2^2 \leq \frac{1}{K} \sum_{i=1}^K |\delta_i|_2^2.$$

857 *Proof sketch.* This is a direct consequence of Jensen's inequality / the variance reduction property of
 858 averaging.
 859

860 **Discussion.** When errors δ_i are approximately zero-mean and weakly correlated, ensembles can
 861 substantially reduce the magnitude of systematic errors that policies can exploit. Worst-case ensemble
 862 strategies (e.g., conservative lower-bound ensembles) further limit reward overestimation.
 863

864
865

A.7 POLICY INITIALIZATION AND RESET STRATEGIES

866
867

Let π_{θ_0} denote a base supervised fine-tuned (SFT) policy. Let us define the Kullback–Leibler divergence between two policies by $D_{\text{KL}}(\pi_{\theta} \parallel \pi_{\theta_0})$.

868
869
870
871
872

Proposition A.6 (Resetting bounds policy drift). *If at every iteration the policy optimisation is initialized from the base policy π_{θ_0} (i.e. we re-start optimisation from θ_0), then the accumulated divergence from the base policy over iterations is bounded by the per-iteration optimisation step sizes. In contrast, warm-starting from the previous iterate θ_{t-1} can lead to cumulative drift: divergences can add across iterations and become large.*

873
874
875

Discussion. Resetting is an effective empirical safeguard against runaway behaviour and can improve reproducibility at the cost of reduced per-iteration adaptivity.

876
877

A.8 OVEROPTIMISATION (ERROR-TO-GAP) BOUND

878
879
880

Proposition A.7 (Error-to-gap bound). *Suppose the reward model approximation error is uniformly bounded: for all outputs y , $|R_{\phi}(y) - R^*(y)| \leq \varepsilon$.*

881
882

Then the suboptimality gap in the maximized rewards satisfies

883
884

$$\max_y R^*(y) - \varepsilon \leq \max_y R_{\phi}(y) \leq \max_y R^*(y) + \varepsilon.$$

885
886
887
888

Discussion. Bounding the sup-norm error of the reward model controls the extent to which an optimiser can overestimate the true reward. The preceding propositions (aggregation and ensembling) are practical mechanisms for reducing ε and hence for limiting overoptimisation.

889
890

A.9 CONCLUDING REMARKS

891
892
893
894
895
896
897
898
899
900
901
902
903
904
905
906
907
908
909
910
911
912
913
914
915
916
917

Framing iterated RLHF as a performative prediction problem clarifies both desirable algorithmic choices and structural failure modes. Under favourable convexity and Lipschitz conditions one recovers a contraction argument guaranteeing convergence to a unique performatively stable reward model. In realistic RLHF pipelines these conditions fail, but the theory explains why mitigation strategies—data aggregation, reward model ensembles, and policy resets—improve stability: they reduce estimation variance, shrink reward-model error, and bound policy drift. Together these tools help iterated RLHF approximate performatively stable equilibria in practice, even when exact theoretical conditions are not met.

918 B REWARD MODEL COMPARISON WITH THE MAXIMUM MEAN DISCREPANCY
919

920 Formally, our goal is to compare any two reward functions R_{ϕ_1} and R_{ϕ_2} . As the first step, we scale
921 both reward functions to have mean zero and variance one. This ensures that reward functions, which
922 differ only by an affine transformation, are treated as equal to one another after scaling. For details
923 about this result, please refer to Appendix B.1. This is desirable since affine transformations do not
924 affect the ordering over policies induced by the original and transformed reward functions when they
925 are optimised Skalse et al. (2024).

926 As the second step, we compute the discrepancy between R_{ϕ_1} and R_{ϕ_2} . While we have reward
927 functions in principle, during training, only samples of rewards from the true and proxy are observed.
928 Given that prompts are identically and independently distributed $x_i \stackrel{i.i.d.}{\sim} \rho$ and $y_i \sim \pi_\theta(\cdot|x_i)$, we
929 obtain that the observed rewards $r_i = R_\phi(x_i, y_i)$ are i.i.d samples (details in Appendix B.1). As a
930 consequence, we can rely on the Maximum Mean Discrepancy (MMD) to measure the discrepancy
931 between distributions of observed rewards from R_{ϕ_1} and R_{ϕ_2} . The MMD compares two distributions
932 based on their distances in the feature space determined by the chosen kernel. It is known for its
933 strong theoretical guarantees, and it is commonly used in the two sample testing literature (Gretton
934 et al., 2012). We use the popular squared exponential kernel.

935 Given samples $\mathbf{r}_{\phi_1} := \{r_{\phi_1,1}, \dots, r_{\phi_1,n}\}$ and $\mathbf{r}_{\phi_2} := \{r_{\phi_2,1}, \dots, r_{\phi_2,n}\}$ an unbiased empirical estimate
936 of the MMD is obtained by

$$938 \quad \text{MMD}_u^2[\mathbf{r}_{\phi_1}, \mathbf{r}_{\phi_2}] = \frac{1}{n(n-1)} \sum_{i=1}^n \sum_{j \neq i}^n k(r_{\phi_1,i}, r_{\phi_1,j}) \\ 939 \quad + \frac{1}{n(n-1)} \sum_{i=1}^n \sum_{j \neq i}^n k(r_{\phi_2,i}, r_{\phi_2,j}) \\ 940 \quad - \frac{2}{n^2} \sum_{i=1}^n \sum_{j=1}^n k(r_{\phi_1,i}, r_{\phi_2,j}).$$

941 Note here that observations \mathbf{r}_{ϕ_1} and \mathbf{r}_{ϕ_2} cannot be assumed to be independent, since when comparing
942 reward models across iterations and proxy reward models with the gold reward model, independence
943 is not guaranteed.

944 This two-step procedure allows us to perform a detailed comparison of reward models going beyond
945 the measurement of the mean gold reward.

946 B.1 PROOFS
947

948 **Proposition B.1.** *Let $R_{\phi_1}, R_{\phi_2} \in \mathcal{R}$ be two reward functions and suppose they differ by an affine
949 transformation, i.e., $R_{\phi_2} = a \cdot R_{\phi_1} + b$ for some $a \in \mathbb{R}^+$ and $b \in \mathbb{R}$. Then $R_{\phi'_1} = R_{\phi'_2}$, where
950 $R_{\phi'_i} = \frac{1}{\sigma_i} \cdot (R_{\phi_i} - \mu_i)$ with σ_i the standard deviation of R_{ϕ_i} and μ_i the mean.*

951 **Proof of Proposition B.1.** First note that $R_2 = a' \cdot R'_1 + b'$, with $a' = a \cdot \sigma_1 \in \mathbb{R}^+$ and $b' = b + a \cdot \mu_1$.
952 We have that $\mu_2 = \mathbb{E}(R_2) = b'$ and $\sigma_2 = a'$. Hence

$$953 \quad R'_2 = \frac{R_2 - \mu_2}{\sigma_2} \tag{4}$$

$$954 \quad = \frac{R_2 - b'}{a'} \tag{5}$$

$$955 \quad = \frac{a' R'_1 + b' - b'}{a'} \tag{6}$$

$$956 \quad = R'_1. \tag{7}$$

957 **Proposition B.2.** *Given i.i.d. observations x_1, \dots, x_n from random variable $x \sim \rho$, and a policy π_θ ,
958 we have that observations of rewards r_1, \dots, r_n , where $r_i = R_\phi(x_i, y_i)$ for a deterministic reward
959 function R_ϕ and $y_i \sim \pi_\theta(\cdot|x_i)$ for $i = 1, \dots, n$, are i.i.d. observations of a random variable we
960 denote by Z .*

972 **Proof of Proposition B.2.** Given that X_i are independent and identically distributed (i.i.d.) and
 973 that $Y_i \sim \pi(\cdot | X_i)$, we first show that Y_i are i.i.d..
 974

975 To determine if Y_i are independent, we need to check if the joint distribution of any pair (Y_i, Y_j) for
 976 $i \neq j$ factorizes into the product of their marginal distributions.
 977

978 Since X_i are i.i.d., we have:
 979

$$P(X_i, X_j) = P(X_i)P(X_j) \text{ for } i \neq j.$$

981 Given $Y_i \sim \pi(\cdot | X_i)$, Y_i and Y_j are conditionally independent given X_i, X_j for $i \neq j$ and the
 982 conditional distribution of Y_i given X_i is independent of X_j for $j \neq i$, such that
 983

$$P(Y_i, Y_j | X_i, X_j) = P(Y_i | X_i)P(Y_j | X_j)$$

985 Using the law of total probability, the joint distribution $P(Y_i, Y_j)$ can be written as
 986

$$P(Y_i, Y_j) = \iint P(Y_i, Y_j | X_i, X_j)P(X_i, X_j) dX_i dX_j.$$

990 Substituting the factored form of the conditional and marginal distributions, we get
 991

$$P(Y_i, Y_j) = \iint P(Y_i | X_i)P(Y_j | X_j)P(X_i)P(X_j) dX_i dX_j.$$

994 Since $P(X_i)$ and $P(X_j)$ are independent, this simplifies to
 995

$$P(Y_i, Y_j) = \left(\int P(Y_i | X_i)P(X_i) dX_i \right) \times \left(\int P(Y_j | X_j)P(X_j) dX_j \right). \quad (8)$$

999 (9)

1001 This shows that
 1002

$$P(Y_i, Y_j) = P(Y_i)P(Y_j),$$

1003 which means Y_i and Y_j are independent for $i \neq j$.
 1004

1005 We now check if Y_i are identically distributed. Since $Y_i \sim \pi(\cdot | X_i)$ and X_i are i.i.d., the marginal
 1006 distribution of Y_i is obtained by marginalizing over X_i , which yields
 1007

$$P(Y_i = y) = \int P(Y_i = y | X_i = x)P(X_i = x) dx.$$

1010 Given that X_i are identically distributed, the distribution $P(X_i)$ is the same for all i . Therefore, the
 1011 marginal distribution $P(Y_i)$ is the same for all i , indicating that Y_i are identically distributed.
 1012

1013 Now, given $R_i = r(X_i, Y_i)$ where r is some deterministic function, we need to determine whether
 1014 R_i are i.i.d., given that X_i are i.i.d. and $Y_i \sim \pi(\cdot | X_i)$.
 1015

1016 Since X_i are i.i.d., X_i and X_j are independent for $i \neq j$. We have established that Y_i and Y_j are
 1017 also independent for $i \neq j$. Because r is a deterministic function, R_i is fully determined by (X_i, Y_i) .
 1018 Specifically

$$R_i = r(X_i, Y_i) \text{ and } R_j = r(X_j, Y_j).$$

1019 Given that (X_i, Y_i) and (X_j, Y_j) are independent pairs, it follows that R_i and R_j are also independent.
 1020 This is because the independence of (X_i, Y_i) and (X_j, Y_j) implies that the mapping through r does
 1021 not introduce any new dependency between R_i and R_j .
 1022

1023 Next, we need to check if R_i are identically distributed. Since X_i are i.i.d. and $Y_i \sim p(\cdot | X_i)$, the
 1024 distribution of (X_i, Y_i) is the same for all i . The function r is deterministic and applies the same
 1025 transformation to each pair (X_i, Y_i) . Therefore, the distribution of $R_i = r(X_i, Y_i)$ will be the same
 for all i . This concludes the proof.

1026 **C ADDITIONAL EXPERIMENTAL DETAILS**
10271028 **C.1 HYPERPARAMETERS**
10291030 Our hyperparameter settings mostly align with those used by the authors in Coste et al. (2024). The
1031 parameters for supervised fin-tuning are given in Table 1, reward model training hyperparameters are
1032 specified in Table 2, PPO parameters are given in Table 3, and the hyperparameters for synthesis with
1033 a policy are provided in Table 4.1034 Table 1: SFT hyperparameters.
10351036

PARAMETER	VALUE
LEARNING RATE	8e - 6
EPOCHS	3
BATCH SIZE	4

1041 Table 2: RM hyperparameters.
10421043

PARAMETER	VALUE
LEARNING RATE	1e - 5
EPOCHS	5
BATCH SIZE	32

1048 Table 3: PPO hyperparameters.
10491050

PARAMETER	VALUE
LEARNING RATE	1e - 6
COSINE ANNEALING SCHEDULER	1e - 7
PPO STEPS	6000
BATCH SIZE	32
NUMBER OF ROLLOUTS	256
CHUNK SIZE	32
CLIPPING RANGE & VALUE	0.2
GAE LAMBDA	0.95

1060 **C.2 DATASET**
10611062 We use the instructions and inputs contained in the popular AlpacaFarm dataset (Dubois et al., 2023;
1063 Taori et al., 2023). The entire dataset contains 52,000 samples split into "sft" (10k), "preference"
1064 (20k), "unlabeled" (20k), and "val" (2k). We use the "val" split strictly only for validation. The
1065 instructions for the reward model training are sampled from the "preference" split and the instructions
1066 for PPO are sampled from the "unlabeled" split.
10671068 **C.3 PROMPT FORMAT**
10691070 We follow the prompt format used in (Coste et al., 2024; Köpf et al., 2023), which is that of the v2
1071 format used in Open Assistant. It uses special tokens <|prompter|> and <|assistant|>, and
1072 is consistent with the GPTNeOXTOKENIZER class.
10731074 To generate answers the model is prompted with the concatenation of instruction and input (if present),
1075 where inputs begin on a new line. The entire prompt begins with the special token <|prompter|>
1076 and ends with the end-of-text token <|endoftext|> to indicate the end of the instruction followed
1077 by the <|assistant|> token to start generating the answer.1078 In the case of the reward model the prompt should additionally contain an answer to the instruction,
1079 which is appended to the initial prompt and again ended with the <|endoftext|> token. Examples
for both generation and reward modelling are given in Table 5.

Table 4: Generation hyperparameters.

PARAMETER	VALUE
MAX INSTRUCTION LENGTH	520
MAX NEW TOKENS	256
PPO EPOCHS	4
TOP-P	0.9 (1.0 FOR PPO)
TOP-K	0
TEMPERATURE	1.0

Table 5: Example answer generation and reward modelling prompts with proper formatting.

Answer generation prompt	Reward modelling prompt
< prompter >Categorize the following items as either furniture or kitchen items.\nChair, Knife, Fork< endoftext > < assistant >	< prompter >Categorize the following items as either furniture or kitchen items.\nChair, Knife, Fork< endoftext > < assistant > Furniture: Chair, Kitchen: Knife, Fork< endoftext >

C.4 COMPUTATIONAL SETUP AND COST

All experiments were run on a single Nvidia A100. Running the full pipeline consisting of all 3 RLHF steps for 4 iterations takes approximately 35 hours per seed and configuration. Subsequently labelling the results with the 7B gold reward model takes approximately 18h when using an evaluation set of size 2000 and evaluating every 300 steps.

Inference overhead for reward models. Reward model ensembles and WCO incur an inference cost proportional to the number of models K (in our case K models must be evaluated). The number of models to be evaluated grows with each iteration. Weight averaging has the significant advantage of zero inference overhead compared to a single model, as the combination happens in parameter space.

Cost performance trade-offs. We summarise the trade-offs based on our results as follows:

- *Concat Data + From SFT (High Robustness, Moderate Cost Increase):* While the reward model training cost scales linearly for *Concat Data*, it is worth noting that RM training is often faster than the generation and PPO phases of the pipeline. Thus, the overhead of concatenating data is often negligible compared to the cost of a failed run.
- *Take Last + Ensemble/WCO (High Cost):* This has high inference costs during PPO (number of forward passes scales linearly with the iteration) but constant reward model training cost. We observed that for smaller models (70M), the computational overhead of ensembles does not yield relative gains over simple data aggregation. For larger reward models performance is more comparable.
- *Weight Averaging (High Efficiency):* This method has no inference overhead and standard training costs, i.e., it is the most efficient. However, our results show that it is less effective at mitigating overoptimisation than for example *Concat Data*.

Our findings suggest that the cheapest methods (like *Take Last*) often lead to policy collapse or stagnation. Therefore, spending the marginal extra compute on *Concat Data* is likely the most efficient option in the long-run.

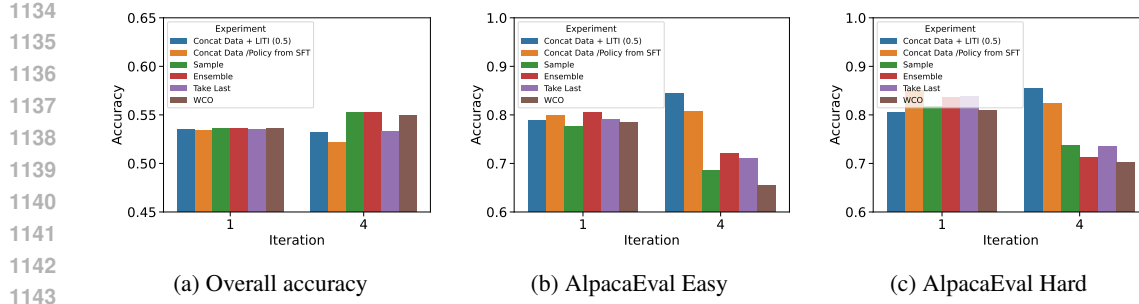


Figure 9: RewardBench performance for 70M reward models.

D FULL REWARD MODEL EVALUATION ON REWARDBENCH

We evaluate the reward models from the first and final iterations that obtained via the different design choices on the reward model benchmark RewardBench (Lambert et al., 2024). In particular, since we train on AlpacaFarm, we report the performance on the AlpacaEval Easy and Hard splits as well as the overall accuracy averaged across all subsets of the benchmark (Figure 9 and Figure 8).

We observe that the proxy reward models, which correspond to methods that ultimately achieve high gold reward in the final iteration, obtain higher or comparable accuracy on the AlpacaEval subsets when comparing the first and final iterations. This is the case for *Concat Data* with the 70 and 160 million reward models, as well as *LITI* with the larger reward model. Interestingly, also *LITI* with the smaller reward model results in performance gains between first and final iteration despite achieving a lower gold reward. We hypothesize that this is due to the concatenation of preference datasets for reward model training. The remaining design choices yield final reward models that achieve lower accuracy on AlpacaEval subsets than their counterparts trained in the initial iteration. The full results of the experiments are also reported in Table 6.

Table 6: RewardBench results grouped by design choice and reward model size.

RM Size	Experiment	Iteration	Accuracy	Alpacaeval Hard	Alpacaeval Easy	Alpacaeval Length
70m	WCO	4	0.550	0.702	0.656	0.588
		1	0.536	0.809	0.786	0.617
	Take Last	4	0.533	0.735	0.711	0.586
		1	0.535	0.838	0.790	0.580
	Sample	4	0.553	0.737	0.686	0.584
		1	0.537	0.817	0.777	0.609
	Ensemble	4	0.553	0.713	0.721	0.591
		1	0.536	0.836	0.806	0.604
	Concat Data /Policy from SFT	4	0.521	0.825	0.807	0.586
		1	0.534	0.851	0.800	0.586
160m	Concat Data + LITI (0.5)	4	0.532	0.855	0.845	0.592
		1	0.536	0.805	0.789	0.584
	WCO	4	0.497	0.809	0.784	0.576
		1	0.439	0.943	0.889	0.534
	Sample Exclusive	4	0.485	0.847	0.797	0.562
		1	0.456	0.917	0.889	0.542
	Sample	4	0.496	0.868	0.845	0.586
		1	0.450	0.932	0.910	0.536
	Ensemble	4	0.496	0.818	0.805	0.567
		1	0.450	0.930	0.882	0.529
	Concat Data /Policy from SFT	4	0.492	0.925	0.914	0.638
		1	0.489	0.941	0.899	0.534
	Concat Data + LITI (0.5)	4	0.482	0.928	0.922	0.632
		1	0.466	0.918	0.886	0.566

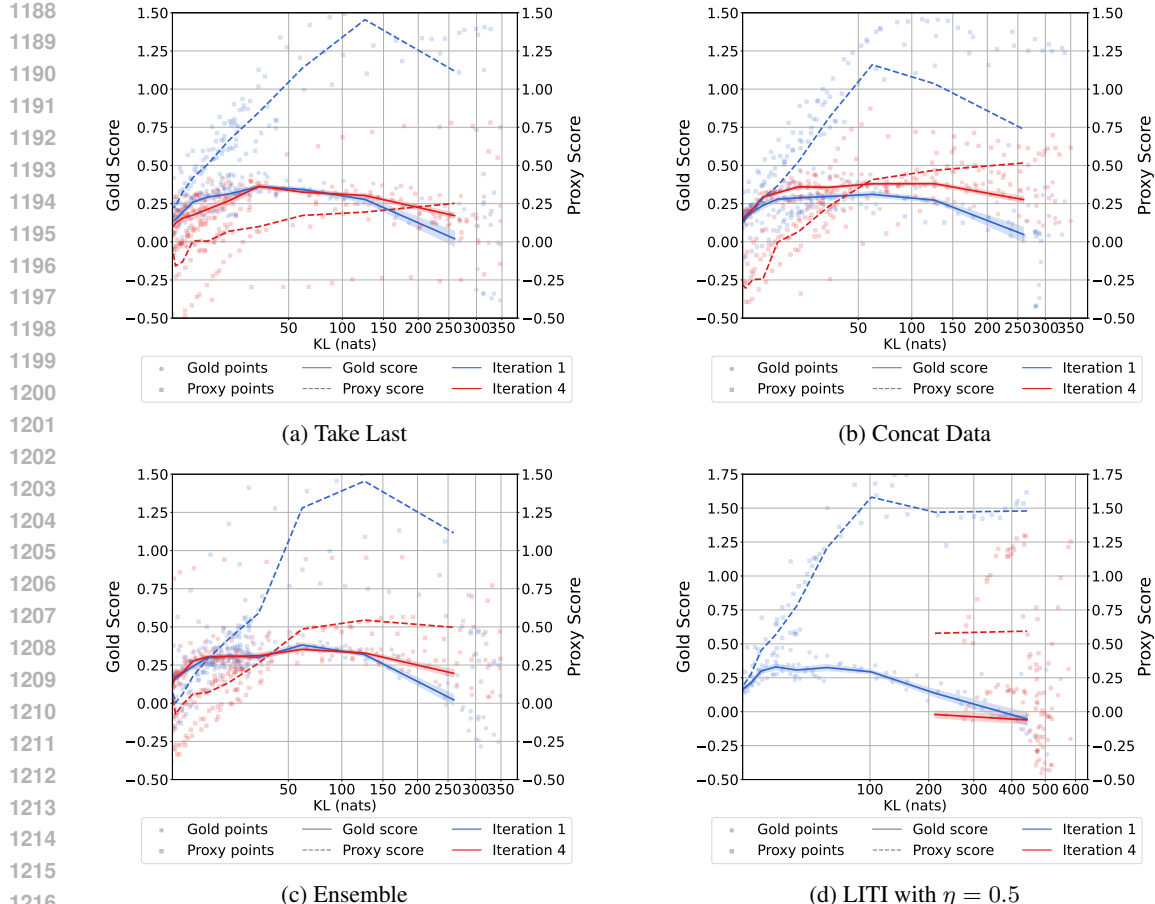
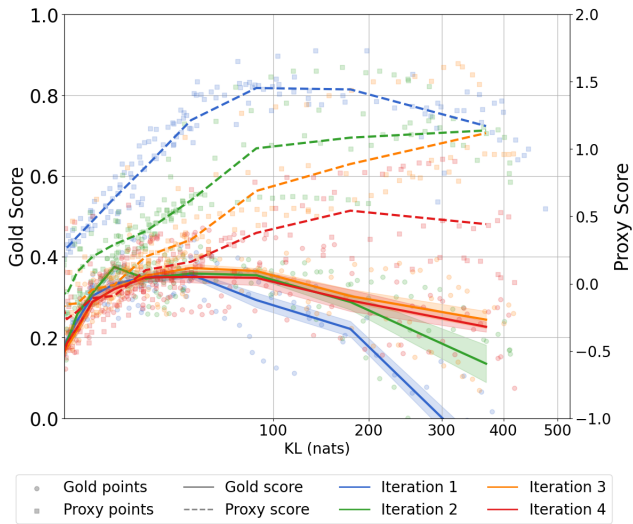
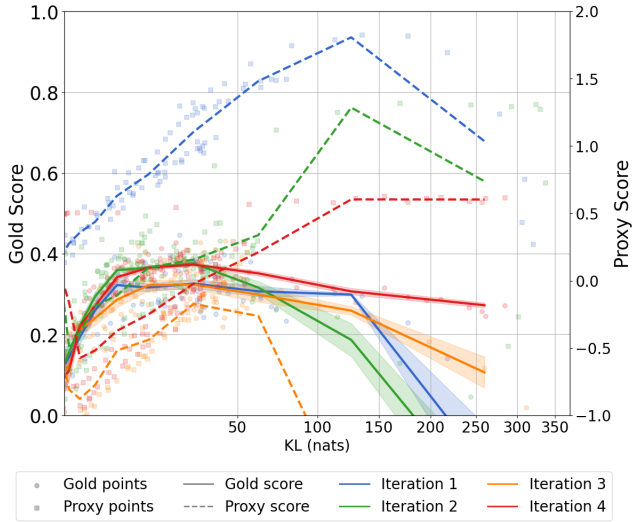
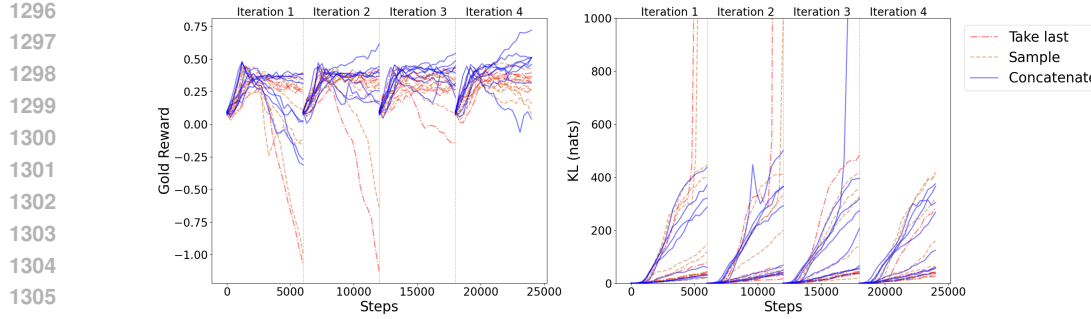


Figure 10: Ablation with 25% label noise in the preference labels the $70m$ reward model is trained on. The hierarchy of design choices as well as the trends across iterations are consistent with the corresponding runs without label noise. Overall, all methods achieve lower gold reward than without label noise, which is expected.

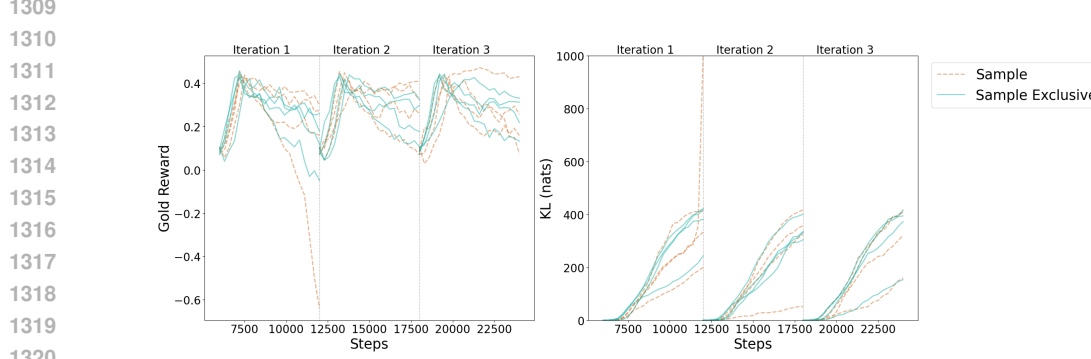
E RESULTS WITH LABEL NOISE

To simulate noisy preference we conduct experiments with 25% label noise. In particular, in the preference labelling phase, each preference label is flipped with probability 0.25. This probability has been found to be empirically consistent with real-world data and has been used to study label noise in prior works (Coste et al., 2024). In Figure 10 we observe that the hierarchy among design choices as well as the trends across iterations are consistent with the results obtained without label noise. We still observe severe overoptimisation in the initial iteration, which some design choice can mitigate towards the final iteration. Additionally, all methods achieve lower gold reward, which is an expected effect of label noise.

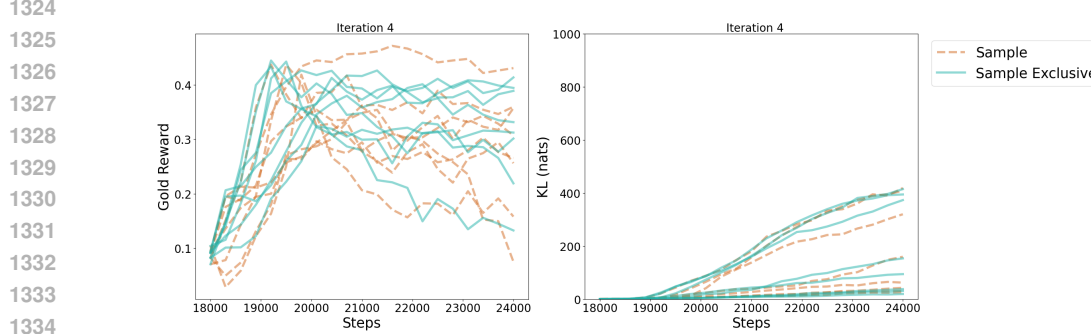
1242 **F ADDITIONAL RESULTS**
12431244 **F.1 CLOSING THE GAP BETWEEN PROXY AND GOLD REWARD FUNCTION**
12451246 Here we provide additional experimental results for taking the last preference dataset and sampling
1247 the preference datasets with equal proportion. In terms of the rate at which the gap between proxy
1248 and gold reward functions is reduced over iterations, the sampling strategy (see Figure 11) falls in
1249 between concatenating all preference data and taking only the last dataset (see Figure 12).
12501268 Figure 11: The gap between gold and proxy reward function when sampling from all preferences
1269 dataset equally to form the reward model training data.
12701288 Figure 12: The gap between gold and proxy reward function when only taking the last preferences
1289 dataset for reward model training.
12901291 **F.2 ADDITIONAL RESULTS FOR COMBINING PREFERENCE DATA**
12921293 In Figure 13 we provide the individual seeds for methods combining preference data across all
1294 iterations and in Figures 14 and 15 we provide the results for the sampling strategies. Figure 16
1295 shows the MMD across iterations when only using the most recent preference dataset.
1296



1307 Figure 13: Gold score and KL of individual seeds across iterations for varying preference data
1308 combination methods.



1321 Figure 14: Gold score and KL of individual seeds across iterations comparing sampling with full
1322 coverage of the prompts vs random sampling.



1335 Figure 15: Gold score and KL of individual seeds in the fourth iteration comparing sampling with
1336 full coverage of the prompts vs random sampling.

F.3 ADDITIONAL RESULTS FOR REWARD MODEL TRANSFER

1342 Here we provide additional results for methods addressing reward model transfer. Figure 17 and 18
1343 show the individual training seeds of the methods across iterations.

F.4 ADDITIONAL RESULTS FOR POLICY INITIALISATION

1348 Here we provide additional results for the policy initialisation methods (Figures 19 and 20). In partic-
1349 ular, we plot the runs associated with each seed, highlighting seeds that are strongly overoptimised
and can not be recovered by the respective methods.

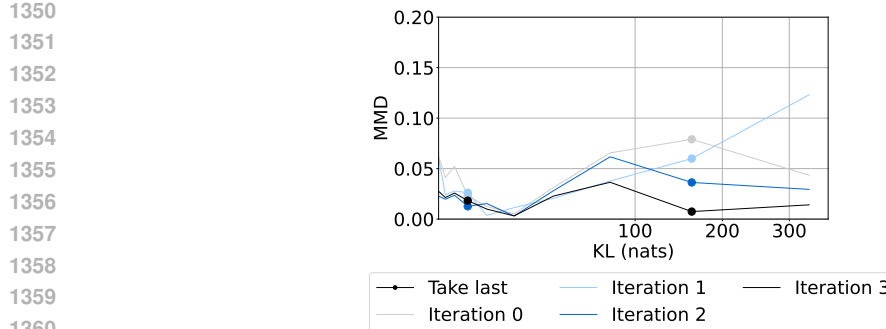


Figure 16: Taking the last preference dataset results in consistently low MMD, in the final iteration.

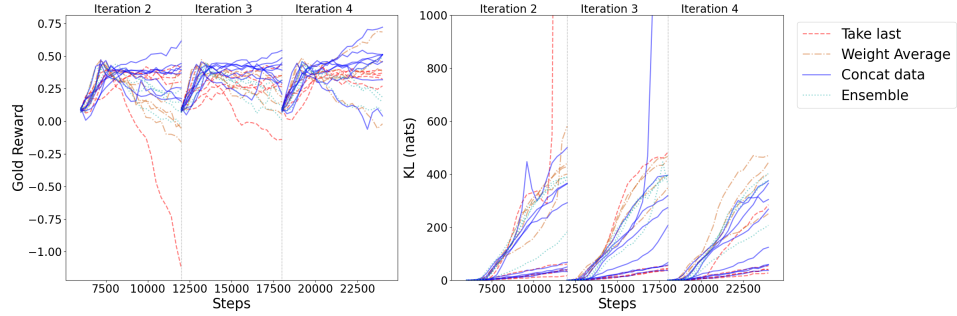


Figure 17: Gold score and KL of individual seeds across iterations comparing reward function choices.

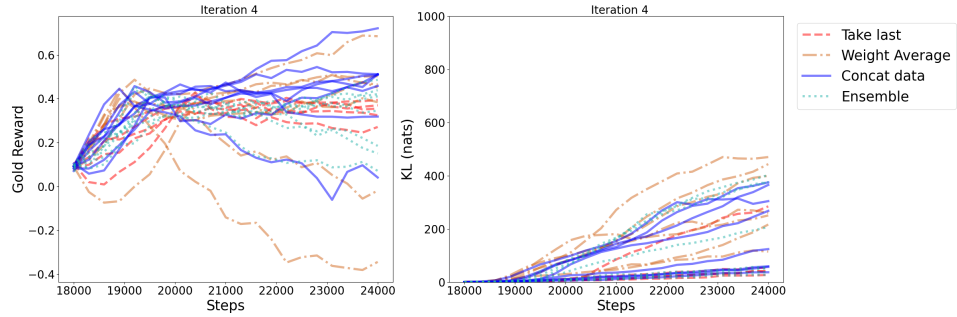


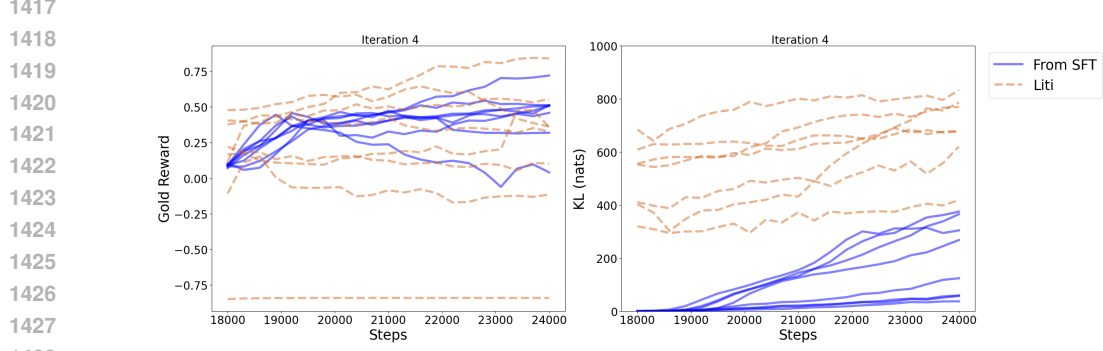
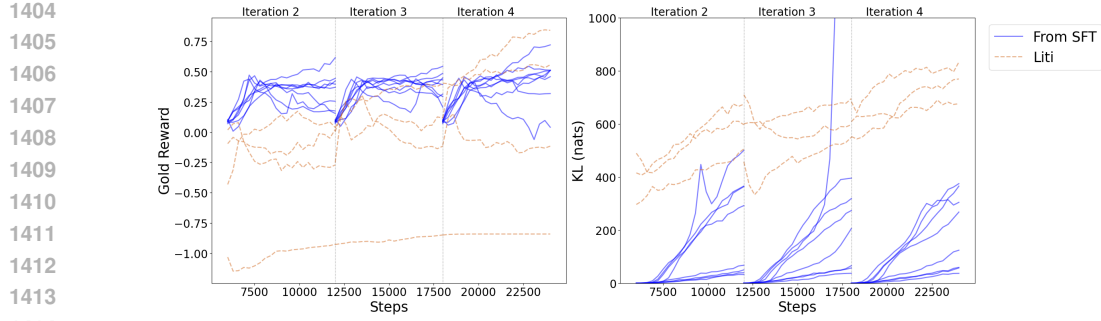
Figure 18: Gold score and KL of individual seeds in the fourth iteration comparing reward function choices.

F.5 INVESTIGATING ENTROPY COLLAPSE

In Figure 21 we show the policy entropy throughout training for the *Take Last* policy initialisation method. The performance collapse extends beyond a simple entropy collapse, suggesting that the policy is exploiting weaknesses in the proxy reward model that cannot be corrected in subsequent iterations.

F.6 ON TRAINING STABILITY ACROSS SEEDS AND ITERATIONS

As is common with RL fine-tuning, we observed variance across random seeds. To mitigate this, we have performed training with 8 random seeds (significantly more than what is standard in the literature) and report the average performance and standard errors. While we focused on the effect of different methods on overoptimisation, we also observed that the methods proposed, particularly those



1431
1432
1433 that reduce overoptimisation, tend to lead to more stable training. For instance, From SFT policy
1434 initialization consistently showed lower variance in performance compared to other initialization
1435 strategies, suggesting improved stability. Please find a summary of these results in Table 7

1436
1437 Table 7: Mean and standard deviation across seeds at the end of the fourth iteration.
1438

1439
1440
1441
1442
1443
1444
1445
1446
1447
1448
1449
1450
1451

Method	Mean	Standard Deviation
Take last Data	0.3572	0.0406
Sample	0.2761	0.0381
Concat Data / Policy from SFT	0.4477	0.0653
Ensemble	0.3136	0.0515
Worst-Case Optimisation	0.2942	0.0450
Weight Average	0.3035	0.1248
Concat Data + LITI	0.1991	0.1678
Sample + Take last Policy	-0.0632	0.1055

G AN EXAMPLE OF IDIOSYNCRATIC BEHAVIOUR

1452
1453
1454 Below we compare example responses from the *Take Last* and *From SFT* Policy initialisation methods
1455 at the start of training and at the end of the fourth iteration. The response at the end of training
1456 obtained with *Take Last* initialisation is notably more repetitive indicating severe overoptimisation.
1457 On the other hand, while still slightly repetitive, the *From SFT* initialisation results in a more sensible
1458 and less idiosyncratic response.

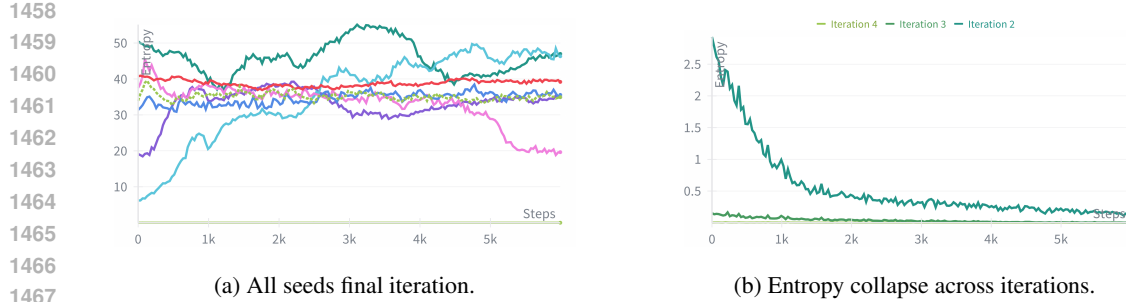


Figure 21: We plot the entropy of the policy against training steps for the *Take Last* policy initialisation strategy. In the final iteration only one out of eight seeds has collapsed.

1488 *Take Last Initialisation*

1489

1490

1491 **Instruction:**

1492 “Given the following input, construct a creative story.

1493 A magic bow and arrow”

1494

1495 **Response from π^{sft} :**

1496 “The Arrow of time was a powerful magical weapon that could grant the user special abilities. It

1497 could grant them the ability to change shape, fly, and even beamed down with sound. The Arrow

1498 of time could also be used to travel to distant lands, granting the user access to magical items and secrets.”

1499

1500 **Response at the end of iteration 4:**

1501 “The story demonstrates the power and ability the ability to use the creativity and the practice in the

1502 practice and the practice in the creativity. This example demonstrates the ability to practice the practice

1503 in the practice in the practice. This demonstrates the practice in the practice in the practice in the

1504 practice. This demonstrates the practice in the practice in the practice in the practice. This demonstrates

1505 the practice in the practice in the practice in the practice. This demonstrates the practice in the practice

1506 in the practice in the practice. This demonstrates the practice in the practice in the practice in the

1507 practice. This demonstrates the practice in the practice in the practice in the practice. This demonstrates

1508 the practice in the practice in the practice in the practice. This demonstrates the practice in the practice

1509 in the practice in the practice. This demonstrates the practice in the practice in the practice in the

1510 practice. This demonstrates the practice in the practice in the practice. This demonstrates the practice in the

1511 practice in the practice in the practice. This demonstrates the practice in the practice in the practice. This demonstrates”

1512

Concat Data and From SFT Initialisation

1513

1514

1515

1516

1517

1518

Instruction:

“Given the following input, construct a creative story.

A magic bow and arrow”

Response from π^{sft} :

“The Arrow of time was a powerful magical weapon that could grant the user special abilities. It could grant them the ability to change shape, fly, and even beamed down with sound. The Arrow of time could also be used to travel to distant lands, granting the user access to magical items and secrets.”

Response at the end of iteration 4:

“A young man named Tom had always wanted to explore the world, but he was scared of the unknown. He was determined to learn to use the skills and knowledge he had acquired in the outdoors and to create his own special abilities and abilities. He set off on an adventurous journey and soon found himself on a magical journey to the far away and mystical world of the Grimm. With the help of a mysterious young woman and a powerful and powerful magic, Tom learned to use the bow and arrow and to create his own unique and powerful abilities. He learned to use the skill and knowledge he had gained in the outdoors and to use it to help protect and help others. This story will inspire and engage readers and will help them to explore and develop their creativity and knowledge in the world of the imagination.”

1520

1521

1522

1523

1524

1525

1526

1527

1528

1529

1530

1531

1532

1533

1534

1535

1536

1537

1538

1539

1540

1541

1542

1543

1544

1545

1546

1547

1548

1549

1550

1551

1552

1553

1554

1555

1556

1557

1558

1559

1560

1561

1562

1563

1564

1565